PB84-122910

Exhaust Emissions from a Diesel Engine

Johns Hopkins Univ., Baltimore, MD

Prepared for

Environmental Sciences Research Lab.
Research Triangle Park, NC

Nov 83

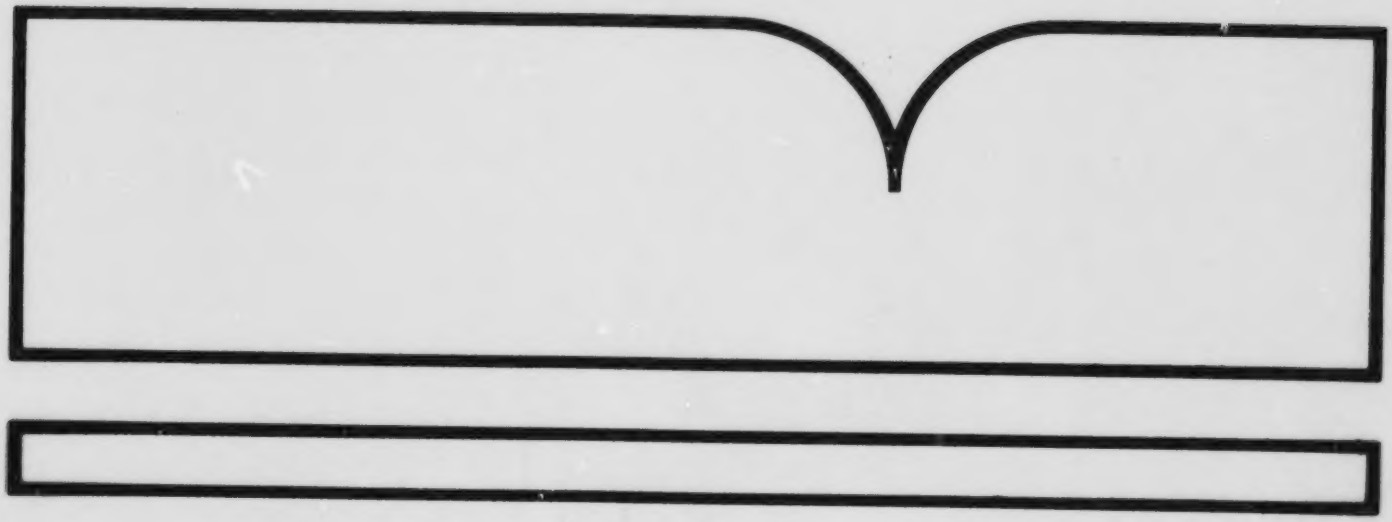

U.S. Department of Commerce
National Technical Information Service
NTIS

TECHNICAL REPORT DATA
(Please read Instructions on the reverse before completing)

1. REPORT NO. EPA-600/3-83-106	2.
3. RECIPIENT'S ACCESSION NO. PB84 122910	
4. TITLE AND SUBTITLE EXHAUST EMISSIONS FROM A DIESEL ENGINE	5. REPORT DATE November 1983
	6. PERFORMING ORGANIZATION CODE
7. AUTHOR(S) Terence H. Risby	8. PERFORMING ORGANIZATION REPORT NO.
9. PERFORMING ORGANIZATION NAME AND ADDRESS John Hopkins University, School of Hygiene & Pub. Hlth. Div. of Environmental Chemists Dept. of Environmental Health Science Baltimore, MD. 21205	10. PROGRAM ELEMENT NO. C9YA1C/01-0442 (FY-83)
	11. CONTRACT/GRANT NO. R-806558
12. SPONSORING AGENCY NAME AND ADDRESS Environmental Sciences Research Laboratory - RTP, NC Office of Research and Development U.S. Environmental Protection Agency Research Triangle Park, North Carolina 27711	13. TYPE OF REPORT AND PERIOD COVERED Final
	14. SPONSORING AGENCY CODE EPA/600/09
15. SUPPLEMENTARY NOTES	

16. ABSTRACT

Studies were performed using (1) Diesel particles collected from the undiluted exhaust of a single-cylinder engine, operated at constant speed and load, using a binary pure hydrocarbon fuel with air or gas mixture oxidizers, and (2) Diesel particles collected from the diluted exhaust of a multicylinder engine operated on a commercial fuel. The physicochemical properties of the particles were determined by static and dynamic methods. The organic adsorbate was characterized by chromatographic and mass spectrometric procedures and by microbial testing protocols. Electron paramagnetic resonance spectrometry and high performance liquid chromatography were used to study reactivity of the organic adsorbate.

The particles collected from the exhaust of Diesel engines operated on binary pure hydrocarbons and on commercial fuels contained similar compounds in the organic adsorbates. The nitrogen in these compounds is derived mainly from the oxidizer (Air).

The microbial mutagenic activities of the organic adsorbates found on the surface of both types of Diesel particles are comparable. These microbial mutagenic activities can be attributed mainly to the presence of nitrated polynuclear aromatic hydrocarbons.

17. KEY WORDS AND DOCUMENT ANALYSIS

a. DESCRIPTORS	b. IDENTIFIERS/OPEN ENDED TERMS	c. COSATI Field/Group

18. DISTRIBUTION STATEMENT RELEASE TO PUBLIC	19. SECURITY CLASS *(This Report)* UNCLASSIFIED	21. NO. OF PAGES 113
	20. SECURITY CLASS *(This page)* UNCLASSIFIED	22. PRICE

EPA Form 2220-1 (Rev. 4-77) PREVIOUS EDITION IS OBSOLETE

PB84-122910

EPA-600/3-83-106
November 1983

EXHAUST EMISSIONS FROM A DIESEL ENGINE

by

Terence H. Risby
Johns Hopkins University School of Hygiene and Public Health
Baltimore, Maryland 21205

EPA Grant Number R-806558

Project Officer

John E. Sigsby
Emissions Measurement and Characterization Division
Environmental Sciences Research Laboratory
Research Triangle Park, North Carolina 27711

REPRODUCED BY
NATIONAL TECHNICAL
INFORMATION SERVICE
U.S. DEPARTMENT OF COMMERCE
SPRINGFIELD, VA. 22161

ENVIRONMENTAL SCIENCES RESEARCH LABORATORY
OFFICE OF RESEARCH AND DEVELOPMENT
U.S. ENVIRONMENTAL PROTECTION AGENCY
RESEARCH TRIANGLE PARK, NORTH CAROLINA 27711

NOTICE

This document has been reviewed in accordance with U.S. Environmental Protection Agency policy and approved for publication. Mention of trade names or commercial products does not constitute endorsement or recommendation for use.

ABSTRACT

Studies were performed using (1) Diesel particles collected from the undiluted exhaust of a single-cylinder engine, operated at constant speed and load, using a binary pure hydrocarbon fuel with air or gas mixture oxidizers, and (2) Diesel particles collected from the diluted exhaust of a multicylinder engine operated on a commercial fuel. The physicochemical properties of the particles were determined by static and dynamic methods. The organic adsorbate was characterized by chromatographic and mass spectrometric procedures and by microbial testing protocols. Electron paramagnetic resonance spectrometry and high performance liquid chromatography were used to study reactivity of the organic adsorbate.

The particles collected from the exhaust of Diesel engines operated on binary pure hydrocarbons and on commercial fuels contained similar compounds in the organic adsorbates. The nitrogen in these compounds is derived mainly from the oxidizer (Air).

The microbial mutagenic activities of the organic adsorbates found on the surface of both types of Diesel particles are comparable. These microbial mutagenic activities can be attributed mainly to the presence of nitrated polynuclear aromatic hydrocarbons.

Table of Contents

Abstract iii
List of Figures vi
List of Tables vii
Acknowledgments viii
Introduction 1
Conclusions and Recommendations 2
Research Report 6
A. Engineering 6
Introduction 6
Experimental 10
Procedures 15
Results 18
B. Chemistry 26
1. Chemical Analysis of Organic Adsorbates 26
Introduction 26
Experimental 27
Results 35
2. Physicochemical Properties of Diesel Particulate Matter ... 45
a. Static Methods 45
Introduction 45
Experimental 46
Results 47
b. Dynamic Methods 65
Introduction 65
Experimental 66
Results 67
3. Transformation of Diesel Particulate Matter 74
Introduction 74
Electron Paramagnetic Resonance Spectrometry 75
Experimental 75
Results 76
Formation of 1-nitropyrene by Reaction of Nitrogen Dioxide with Diesel Particulate Matter 83
Experimental 83
Results 83
C. Biology 85
Introduction 85
Experimental 85
Results 91
Conclusions 98
References 99
List of Publications which have resulted from this research 104

List of Figures

Figure		Page
1	Exhaust System	13
2	Gas Phase Instrumentation	14
3	Pressure Traces	21
4	Carbon Monoxide and Unburnt Hydrocarbons as a function of Oxygen	22
5	Nitric Oxide and Nitrogen Dioxide as a function of Oxygen	24
6	Ignition Delay, Particulate, and Extract as a function of Oxygen	25
7	Block Diagram of Temperature - Programmable Platinum Wire Probe	33
8	Capillary Gas Chromatogram of Air Oxidant Sample using Flame Ionization Detection	36
9	Capillary Gas Chromatogram of Nitrogen-free Oxidant Sample using Flame Ionization Detection	37
10	High Performance Liquid Chromatogram of Air Oxidant Sample	43
11	Volumetric Adsorption Apparatus	48
12	Adsorption Isotherms of Benzene on DPM-PSU (350°C)	52
13	Adsorption Isotherms of Nitrogen on DPM-EPA	54
14	Adsorption Isotherms of Benzene on DPM-EPA	55
15	Heat of Adsorption vs Surface Coverage for Benzene on Spheron 6	58
16	Heat of Adsorption vs Surface Coverage for Benzene on DPM-PSU (350°C)	59
17	Heat of Adsorption vs Surface Coverage for Hexane on DPM-PSU (100°C)	60
18	Heat of Adsorption vs Surface Coverage for High Temperature Benzene Adsorption on DPM-EPA (50°C)	61
19	Heat of Adsorption vs Surface Coverage for Low Temperature Benzene Adsorption on DPM-EPA (50°C)	63
20	Heat of Adsorption vs Surface Coverage for Benzene on DPM-EPA (400°C)	64
21	Gas Chromatographic Log Vr vs 1/Tc Plots for Benzene	68
22	Relative Positions of EPR Signals	77
23	Effects of Various Treatments on the EPR Signals of DPM-PSU	79
24	Nitration System	84

List of Tables

Table		Page
1	Engine Parameters	11
2	Test Conditions	18
3	Engine Data	19
4	Chemical Characterization of Organic Adsorbates on Diesel Particulate Matter	38
5	Concentration of 1-nitropyrene in the Extracts of Particulate Matter collected from Engines Operated on Various Oxidants	44
6	Electron Microscopy Results	49
7	True and Bulk Densities	50
8	B.E.T. Surface Areas	51
9	E.M. *vs* B.E.T. Nitrogen Surface Areas	56
10	Isoteric Heat of Adsorption for Various Graphitized Carbon Blacks	69
11	Variation of Apparent Heats of Sorption with Volume of Adsorbate Injected	72
12	Isosteric Heats of Adsorption	73
13	Line widths and g-Values	76
14	Effects of Various Treatments on the EPR Signals of DPM-PSU	78
15	Effects of Selected Gases on the EPR Signals of DPM-PSU	81
16	Effects of Irradiation on the EPR Signal of DPM-PSU	82
17	Reaction of Nitrogen Dioxide with Nitrogen-free Particulate Matter	85
18	Genotype of the TA Strains used for Mutagen Testing	86
19	Quantitative Ames Mutagenesis Results	92
20	Relative Transformation of Strain RUB 827 to Diesel Particulate Matter	93
21	Percentage Survival of TA 98, TA 100 at Various Doses	94
22	Biological Activity of Used and Unused Lubricant and Model Fuel	95
23	Biological Activity of Particulate Matter Collected from Engine operated with Nitrogen-free Oxidant	96
24	Biological Activity of Particulate Matter Collected from Engine operated with Different Oxidants	97
25	Biological Activity of Particulate Matter after Reactions with Nitrogen Dioxide	98

ACKNOWLEDGMENTS

The principal investigator wishes to acknowledge and thank his collaborators without whose help this project would not have been possible: Professor S.S. Lestz, Professor M.R. Chedekel, Dr. J.A. Yergey, Dr. M.M. Ross, M. Dukovich and J.D. Herr. The investigators would like to express their thanks to J.E. Sigsby, Jr., Dr. R.L. Bradow, Dr. S.B. Tejada, Dr. R.B. Zweidinger, M. Walsh, Esq. and S. Blacker, Esq., of the U.S. Environmental Protection Agency for their advice, help and continued support during the progress of this research. Also we wish to thank Dr. S.R. Prescott and V. Lafferty for allowing us to use their gas chromatograph-electron impact mass spectrometer systems.

INTRODUCTION

A number of studies have reported that the exhaust particulate matter from Diesel engine combustion represents a potential environmental health hazard. These studies were based on the microbial activity of the organic adsorbate which is obtained by the Soxhlet extraction of Diesel particulate matter with dichloromethane. However these *in vitro* results have not been corroborated *in vivo* by animal exposure studies since no measurable effects were obtained in these latter studies. This dichotomy of results is complicated further by other *in vitro* studies which have used certain physiological fluids to extract Diesel particulate matter for microbial assays and have found the extracts to be inactive. A possible explanation is that the positive or negative results are caused by anomalies in the engine operation or from differences in fuels. The chemical composition of Diesel fuel is widely variable and as a result it is difficult to compare results which are obtained with fuels that have the same ignition and boiling point characteristics but different chemical compositions. An even more likely explanation is that the results are different because they involve the use of different samples. The *in vitro* analyses were performed using collected particulate matter and the *in vivo* analyses were performed with diluted Diesel exhaust. The difference may, therefore, be the result of a sampling artifact. In this research we have attempted to address all the variables of fuel, oxidant, lubricant and engine operating parameters and have also made some interesting observations with regard to sampling artifacts. We have also measured the physicochemical properties of Diesel particulate matter and performed some preliminary studies which have addressed the area of photochemical and chemical reactivity of Diesel particulate matter.

CONCLUSIONS AND RECOMMENDATIONS

This final report describes in detail the results that were obtained from this research. These results have major impact on studies evaluating the potential health risks that may be associated with exposure to Diesel particulate matter. The major conclusions to be be drawn from this research are as follows:

1. The compounds that have been identified and quantified as sorbed on the surface of Diesel particulate matter are inherent to the combustion that occurs in the Diesel engine. The same major compounds are found to be sorbed on the particles if the Diesel engine is operated on commercial Diesel fuel or a mixture (1:1 V/V) of n-tetradecane and 2,2,4-trimethylpentane (model) fuel

2. The combustion mechanisms, which lead to the production of the polynuclear aromatic compounds, appear to involve short chain intermediates; this is the only way to explain the formation of similar compounds from different fuels.

3. The microbial activities are comparable for organic adsorbates from particulate matter collected from the exhaust of Diesel engines operated on commercial Diesel fuel (5.5 Rev/µg TA98) or on the model fuel (4.3 Rev/µg TA98).

4. Similar nitrogen cont ining compounds are found sorbed on the particulate matter from engines operated on model fuel or commercial Diesel fuel. The source of nitrogen has been thought to be the fuel or lubricant, but since the model fuel and the synthetic lubricant (polyalkyleneglycol) are nitrogen free the origin of the nitrogen in the engine operated on model fuel must be the intake air.

5. The previous conclusion is confirmed by a study using a nitrogen free model oxidizer intake; the sorbed molecules are found to be nitrogen free. Also the microbial activity of the soluble organic extract of particulate matter collected from the engine operated on this model fuel and oxidizer is reduced by a factor of fifty compared to the engine operated on the model fuel and air.

6. Most of the direct microbial activity of the soluble organic extract can be attributed to nitrated polynuclear aromatic hydrocarbons; including 1-nitropyrene.

7. The microbial activity of the soluble organic extract of particulate matter collected from the engine operated with model fuel and oxidizer can be restored by reacting the particulate matter on a filter with nitrogen dioxide (nitric acid). The microbial activities show direct correlation to the concentration of 1-nitropyrene.

8. The direct correlation between microbial activity and 1-nitropyrene is substantiated further by operating the engine with the model fuel and intake air supplemented with various concentrations of oxygen and nitrogen.

9. The new or used lubricants used for the engine operated on model fuel do not show any microbial activities.

10. Preliminary studies using electron paramagnetic resonance spectrometry show that Diesel particulate matter is photochemically active and will react with other pollutant gases.

11. The mean particle diameter of Diesel particulate matter emitted by the engine operated on the model fuel is found to be 36 nm by electron microscopy; this is similar to the mean diameter of the particles which are collected from an engine operated on commercial Diesel fuel (28 nm).

12. The external surface areas of particles collected from the engine operated on the model fuel are found by electron microscopy to be 86 m^2/g and the external and internal surface areas of the same particles are found by the nitrogen B.E.T. methodology to be 104 m^2/g. The external and total surface area of particles collected from the engine operated on commercial Diesel fuel are identical 112 m^2/g. The difference between these results (if significant) can be explained by the latter particles having a coating of unburnt hydrocarbons or lubricant on their surfaces which decreases the accessibility of nitrogen to the pores of the particle.

13. The isosteric heats of adsorption for a series of model compounds were measured for the particulate samples collected from the engine operated on the model fuel and the engine operated on commercial Diesel fuel. The heats of adsorption are significantly greater for the particulate matter collected from the engine operated on the model fuel owing to the lower coverage by high molecular weight compounds.

14. The variation of the apparent heats of sorption with increase of surface coverage shows the expected decrease in sorption energy. This study also shows that the particles have both high and low energy sorption sites.

15. Sampling conditions are shown to affect the quantity of adsorbates which are present on the surface of the particles.

It is apparent from these results that a number of questions must still be answered in order to establish conclusively whether Diesel particulate matter represents a significant health hazard. The following recommendations summarize the areas for future research which are obvious extensions of this work.

1. Measure the bioavailability of sorbates from the surface of Diesel particles using both <u>in vitro</u> and <u>in vivo</u> testing protocols.

2. Determine the fate of airborne Diesel particles in typical urban atmospheres in terms of photochemical and chemical reactions.

3. Determine the relationship between engine speed and load and the chemical composition of the sorbate on the surface of Diesel particles.

4. Determine whether sampling artifacts play a role in the observed biological activity of Diesel particulate matter. This study could most easily be performed by *in vivo* exposure of animals to reaerosolized Diesel particulate matter, providing that the aerosol has a similar size distribution.

RESEARCH REPORT

This final report will be split, for the sake of clarity, into three areas. (A) Engineering: The generation and collection of Diesel particulate matter. (B) Chemistry: Determination of the physical and chemical properties of the Diesel particulate matter, studying the reactions of the sorbates. (C) Biology: Determination of the biological activity of the particulate matter using various microbial assays.

A. ENGINEERING

INTRODUCTION

Diesel Combustion

The ideal Diesel cycle starts with a reversible isentropic compression: the piston compresses the air in the cylinder. Near top-dead-center fuel is injected into the hot compressed air and combustion is self-initiated. This process is respresented in the ideal cycle as the addition of energy at constant-pressure. At this point the actual process differs from the ideal thermodynamic cycle. When the fuel is first injected into the cylinder, it undergoes an ignition delay - the time between fuel vaporization and the initiation of preflame chemical reactions. Consequently, some of the fuel accumulates and burns at essentially constant-volume. Following ignition, the fuel continues to spray into the combustion chamber, simulating the ideal constant-pressure addition of heat. After the injection of fuel has ceased, the hot gases expand to provide the power stroke of the engine. When the exhaust valve opens, the exhaust gas exits the cylinder. This blowdown process is approximated as a constant specific-volume rejection of heat. However, a real engine does not follow a cycle, since the exhaust gases are expelled and atmospheric air is introduced. Furthermore, the real processes depart from the processes of the ideal cycle in that they are neither

reversible nor isentropic. Therefore, while the ideal Diesel cycle can serve as a model to determine theoretical thermodynamic limits for an engine design, the ideal cycle is of little use in understanding the actual Diesel combustion system.

Combustion in the absence of nitrogen

To simulate the combustion cycle with an oxidizer other than air, several parameters must be maintained. The compression pressure and temperature of both the model oxidizer and air must be comparable in order to achieve similar ignition properties. The peak combustion temperature for the model oxidizer must be close to the peak temperature obtained with air, in order to produce similar combustion products. The temperature and pressure of the oxidizer at the engine inlet should be maintained as close to ambient atmospheric conditions as possible. Constant fuel-to-oxygen ratios must be maintained in the air and the nitrogen-free oxidizer systems, and a constant mass flow rate of oxygen into the engine must be produced. These parameters are governed by a system of thermodynamic, equations and properties of various inert gases and oxygen can be substituted to calculate the composition of a nitrogen-free oxidizer that will simulate air in the combustion cycle.

No single inert diluent was found to satisfy the thermodynamic equations, but they were satisfied by a mixture of carbon dioxide and argon. The actual composition of the nitrogen-free oxidizer was calculated to be as follows: 21% oxygen, 23% argon, and 56% carbon dioxide.

Combustion with Nitrogen- and Oxygen-Enriched Air

The mixture of argon, oxygen and carbon dioxide eliminates nitrogen from the combustion process, but the effects of excess nitrogen and oxygen in the oxidant were also of interest. Therefore, small amounts of excess oxygen or nitrogen were added to the intake charge. Although these additions altered some of the engine parameters the thermodynamic and transport properties of the engine changed vary little(1).

Nitrogen added to the intake charge, simulates exhaust-gas-recirculation (EGR) and this process is known to produce the following effects: reduction in the emission of nitric oxide; increase in the exhaust temperature, and increases in the emissions of particulate matter(1,2,3,4). The reduction in nitric oxide is the reason for interest in Diesel EGR, but the increase in the emission of particulate matter is undesirable. However, the level of the organic adsorbate is not increased by the use of EGR(3).

An increase in the oxygen content of the intake charge has both beneficial and detrimental effects upon the engine. As oxygen is added to the air, the ignition delay becomes considerably shorter, and the rate of pressure rise increases(1,4). Also, the peak cylinder pressure increases until a maximum value is reached at about 38% oxygen(1). In direct contrast to nitrogen addition, excess oxygen decreases the emission of particulate matter and increases the emission of the oxides of nitrogen. Both these emissions are dependent upon the oxygen radical concentration as indicated by the Zeldovich equations:

$$O + N_2 \rightleftharpoons NO + N$$
$$N + O_2 \rightleftharpoons NO + O$$
$$O + NO \rightleftharpoons NO_2$$
$$NO + O_2 \rightleftharpoons NO_2 + O$$

Diesel Exhaust Emissions

Even though all engines emit both gaseous and aerosol products, Diesel engines emit 30 to 50 times more particulate matter than comparable SI engine(5).

Particle Formation

For many years particle emissions have been indicators of Diesel engine performance and condition and have been a main consideration in engine design. Particulate matter, which is an aerosol of carbonaceous particles suspended in the exhaust gas, is a product of incomplete combustion and is commonly called soot or smoke. Although equilibrium equations fail to predict the production of these particles at typical combustion pressures and temperatures, it is always present in the exhaust(6).

Particulate matter is defined as any dispersed matter in the solid or liquid phase present in diluted exhaust gases near ambient conditions(6). These particles may vary from very small, single particles of 10 nm to long clusters in the 10 to 30 μm range(6). The mass of the particulate matter in the exhaust stream is affected by the type of fuel and fuel additives. Increases in the fuel density, the sulfur content or aromatic content increase the emission of particles(2). The ignition delay also affects the particulate emissions since fuels with low cetane numbers yield lower masses of particulate matter. This indicates that longer ignition delays are beneficial, giving the fuel and air more time to mix. However, the gaseous products show little fuel-to-fuel variation. Analysis of the major components of particulate matter shows few differences between the fuels tested(2). The major constituents of the particulate are carbon, hydrocarbons, sulfates, metals, and water(6).

Precombustion chamber engines also emit up to 20% less particles than a comparable direct injection engine(3). Also a difference in the nature of the particulate matter has been observed. The indirect-injection engine produces drier particles which contain more carbon, whereas the direct injection engine produces oily particles characteristic of higher hydrogen-to-carbon ratios(3).

Dilution

As the exhaust products travel down the exhaust pipe the temperature drops and organic molecules sorb and condense on the carbon particles(7,8). Initially, when the temperature is above 200°C, most organic molecules are in the gas phase. This is evident when particulate matter is collected at elevated temperatures, since only 1% of the particulate matter collected at 200°C can be extracted into dichloromethane(8). Other results have shown a drop in the amount extractable from 35% to 20% when the collection temperature of diluted exhaust was increased from 35°C to 100°C (9). The U.S. Environmental Protection Agency has set a maximum of 52°C for the collection of particulate matter. This temperature is sufficient to condense or sorb most of the high molecular weight organic molecules onto the carbonaceous particles(7). Approximately one-third of the total organic molecules in the gas phase are thought to be sorbed onto the particles. These compounds include polynuclear aromatic compounds which may be the origin of the biological activity(10).

The transformation of the collected particulate matter varies widely. Factors such as sedimentation, diffusion to the walls, evaporation, condensation, collision, gain or loss by surface charge, liquid and gas phase reactions, catalysis, surface adsorption, and photochemical reactions will change the chemical and physical properties of the particulate matter(6).

EXPERIMENTAL.

Engine and Dynamometer

The engine used in this study was an AVCO-Lycoming Bernard W-51 industrial Diesel engine. It is a small-single cylinder, four-stroke cycle, air-cooled, direct-injected Diesel engine capable of 3000 revolutions per minute (RPM). Table 1 summarizes some of the engine parameters.

Table 1. Engine Parameters

Engine Speed	2400 ± 25 RPM
Rack	Full
Air Inlet Pressure	760 ± 5 torr
Lubricant Temperature	61 ± 2°C
Injection Timing	27° BTDC
Filter Temperature	51 ± 2°C
Displacement	355.6 mL
Compression Ratio	18:1
Bore	7.62 cm
Stroke	7.78 cm
Rated Power	4.47 bkW at 3000 RPM
Frictional Power	2.14 fkW at 2400 RPM

This engine is directly coupled to a General Electric type TLC-6 cradled electric dynamometer which loads and motors the engine. The dynamometer is used to start the engine and to measure the frictional power. Engine torque output was calculated from the dynamometer balance-beam which has a scale with 0.05 kg subdivisions. The dynamometer equation is as follows:

$$1.0\ \text{bkW} = (\text{Scale Unit.}\ \text{RPM})/8046.$$

Pressure Measurements

A Kristal 601A piezoelectric pressure transducer, mounted in the cylinder head of the engine, monitors the pressure and the output is amplified by a Kiag Swiss Type 5002 charge amplifier. The data are stored on a Nicolet Series 2090 model 206 Explorer digital oscilloscope with a model III magnetic disc memory unit.

Fuel

Since Diesel fuel is manufactured from various crude oils by complex refining processes, a 1:1 mixture by volume of 2,2,4-trimethylpentane and n-tetradecane has been substituted as a model fuel. This mixture has a measured cetane number of 53.4 and this mixture of two pure hydrocarbons was expected to reduce the number of species in the exhaust and thereby simplify its analysis.

To prevent possible contamination of the combustion products with lubricant, polyalkyleneglycol (Ucon LB525 Union Carbide) was used to lubricate the engine. Since this synthetic oil starts to decompose above 71°C, a retrofitted oil cooler was used to maintain an oil operating temperature of 60°C.

Exhaust Emission

In this study both the exhaust particles and gases were of interest and this section describes the hardware and instruments used to monitor and collect the exhaust.

Gas Phase

The gases and particles were continuously sampled via a stainless steel sample probe in the exhaust pipe. The sample probe is shown in Figure 1, and the gas-phase instrumentation is shown in Figure 2. The following exhaust gases were measured: carbon dioxide, carbon monoxide, oxygen, oxides of nitrogen, and unburned hydrocarbons. These gases were measured as described below.

The oxides of nitrogen were measured by a heated chemiluminescent analyzer (Beckman model 955) calibrated with a 550 ppm NO span gas. The oxygen was monitored with an amperometric sensor, (Beckman model 741) calibrated with air. The carbon monoxide and carbon dioxide were

Figure 1. Exhaust System

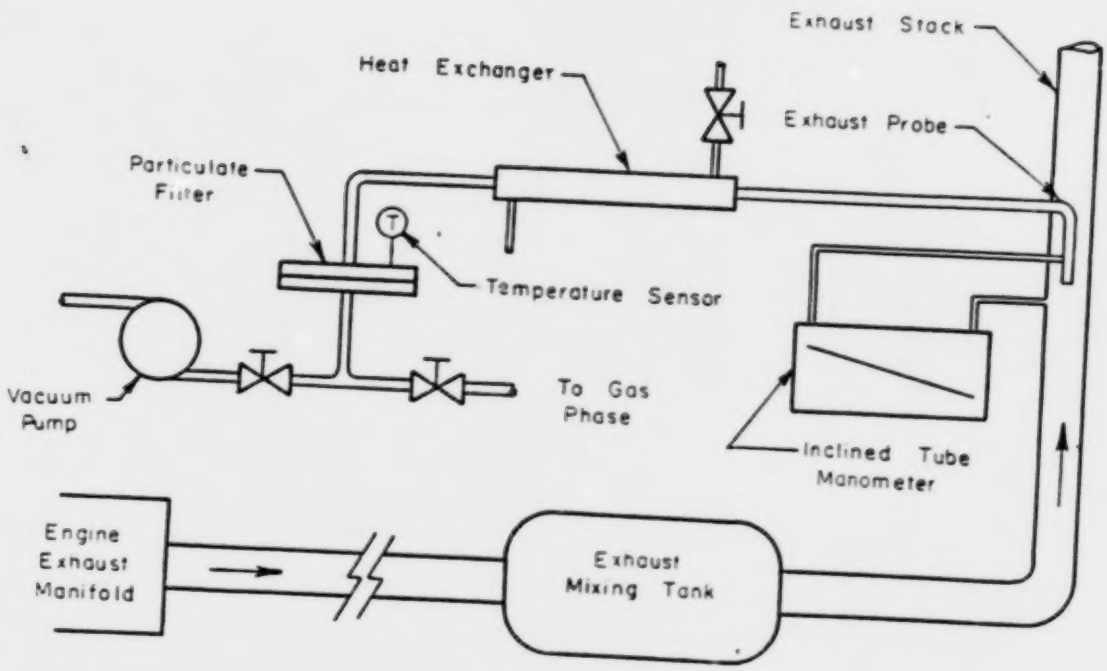

Figure 2. Gas Phase Instrumentation

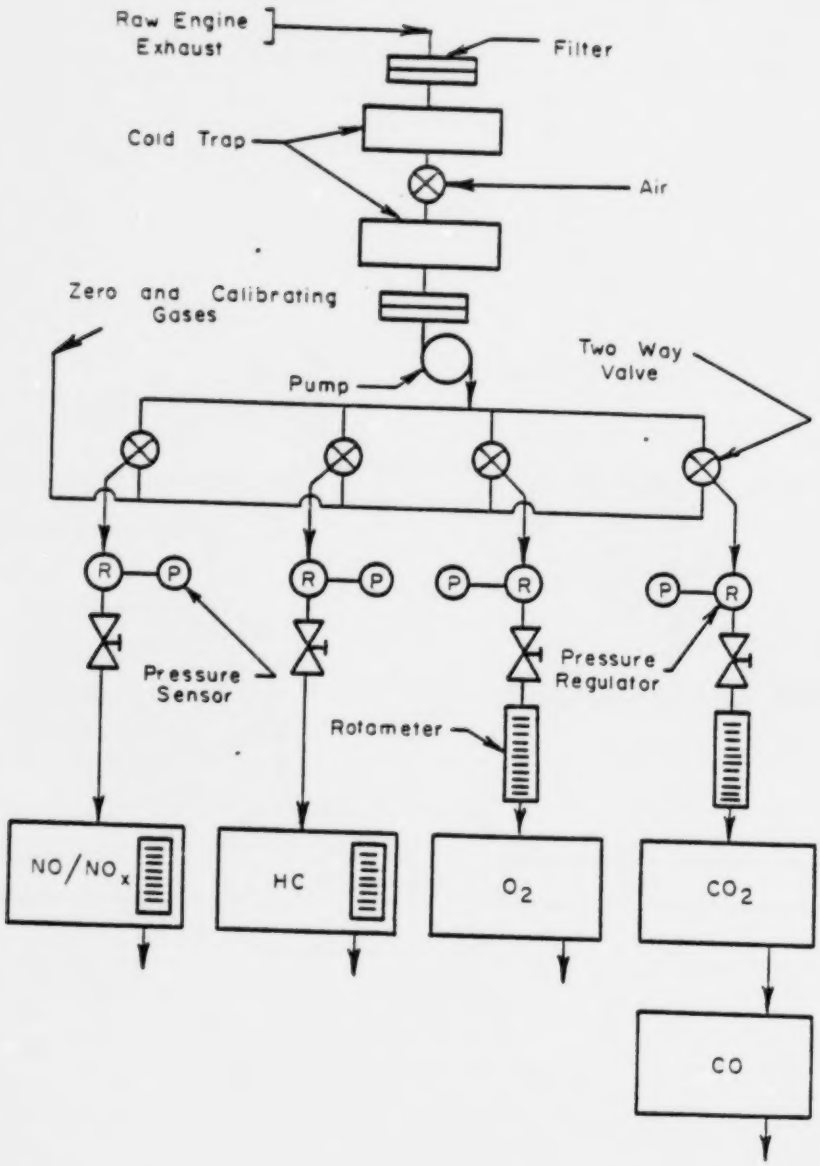

monitored by infrared spectrometers (Beckman type 864 and IR-15A) calibrated with 415 ppm CO and 14.9% CO_2 calibration gases. The unburned hydrocarbons are analyzed with an unheated flame ionization detector (Beckman type 109) calibrated with 530 ppm methane in nitrogen. The line to this latter instrument was heated.

Particulate Matter

Particles were collected on Teflon-coated, glass-fiber filters (Pallflex type T60A20). These filters are expected to collect at least 90% of Diesel particles and were contained in a stainless steel sample holder. The stainless steel sample probe (10.7mm id) is located in the exhaust stack (40.9mm id). The flow is turbulent at all locations in the exhaust stack and therefore a representative sample is ensured(11).

Since the raw exhaust is not diluted with air, the heat exchanger was used to cool the exhaust to 51.7°C. The exhaust gas temperature drops approximately 100°C in the heat exchanger, thereby condensing high molecular weight compounds onto the carbon particles.

The difference in total pressure between the sample probe and the exhaust stack was monitored continuously. The static pressure difference indicates the differential dynamic pressure. The valve on the vacuum pump was adjusted to ensure that a constant pressure drop (and thus velocity and flow rate) was maintained in the sample line during filter loading. Approximately 17% of the combustion products were sampled through the probe.

PROCEDURES

The object of this study is to discern the effect of various inlet oxidizers upon the particulate matter. For all conditions the engine was operated at full rack, 2400 RPM, with the 1:1 fuel mix of n-tetradecane and 2,2,4-trimethylpentane.

Nitrogen-Free Oxidant

The nitrogen-free oxidizer consisted of a mixture of gases (21% oxygen, 23% argon, and 56% carbon dioxide) which simulated air in the Diesel combustion cycle. It was assumed that the volumetric efficiency of the engine is independent of gas composition and a calibrated intake rotameter was used to ensure that a flow equal to that of air entered the engine.

One problem with this gas mixture is that under pressure the carbon dioxide liquifies and settles to the bottom of the cylinders. As a result, a gas mixture which is rich in argon and oxygen is produced that does not have the desired thermodynamic properties. This problem was solved by agitating the cylinders, wrapping them with heating tapes, and heating above 31°C, the critical temperature of carbon dioxide.

Another drawback of this mixture is that the high concentration of carbon dioxide increases the ignition delay to such an extent that the engine did not run. When the injection timing was advanced it caused the engine to knock and to operate roughly. This problem was rectified by the addition of oxygen into the intake manifold until the engine ran smoothly. The oxygen which was added was approximately 10% of the baseline-air flow and the flow of the nitrogen-free gas was 90% of the baseline-air flow. Therefore, the actual gas, which entered the engine, was maintained at standard conditions, and had a composition of 28.9% O_2, 20.7% Ar, and 50.4% CO_2.

Air Supplemented with Nitrogen or Oxygen

The effects of excess oxygen and nitrogen upon the chemistry of the particulate matter were also of interest and these studies were performed by supplementing the engine with excess oxygen or nitrogen. Since only 5% and 10% of additional nitrogen or oxygen were used, negligible effects on the engine or its operating conditions were observed.

In supplementing the air with nitrogen the amount of oxygen was held constant, so the fuel to oxygen ratio was the same as the baseline condition, but, the mass of the diluent (nitrogen) increases. Supercharging the engine with 5% and 10% nitrogen results in the intake charges being composed of 20.0% and 19.1% oxygen by volume, respectively. Since the ratio of specific heats for nitrogen is 1.4, the compression process remains constant although increases in the intake manifold pressure of 0.031 and 0.062 bar, respectively, were measured.

When the air was supplemented with 5% or 10% oxygen the flow rate of nitrogen remains constant and the composition intake charge is 24.8% and 28.2% oxygen, respectively. The ratio of specific heats for oxygen is also about 1.4. The test conditions are outlined in Table 2.

Filters

Exhaust gas was sampled for 10 to 25 minutes, depending upon the loading rate. The optimum mass of particulate matter on each filter was found to be in the range of 0.1 to 0.2g since after a loading of 0.2g the pressure drop across the filter becomes too large. The filters were placed in a desiccator for 24 hours before they were weighed. Also the filters were protected from light to prevent photochemical reactions and refrigerated to prevent any reactions until they were extracted and analyzed.

The organic adsorbates were removed by the Soxhlet extraction with dichloromethane for 24 hours at a rate of two cycles per hour. The majority of the solvent was removed by a rotary evaporator and the extract was blown to final dryness with dry nitrogen or argon. Finally, the extract was sealed in a vial, protected from light, and refrigerated.

Table 2. Test Conditions

Test	RPM	Load	Inlet Oxidizer	Composition
1	2400	Full	Air	21.0% O_2, 79.0% N_2
2*	2400	Full	N_2-Free	21.0% O_2, 23.0% Ar 56.0% CO_2
3	2400	Full	Air+5% N_2	20.0% O_2, 80.0% N_2
4	2400	Full	Air+10% N_2	19.1% O_2, 80.9% N_2
5	2400	Full	Air+5% O_2	24.8% O_2, 75.2% N_2
6	2400	Full	Air+10% O_2	28.2% O_2, 71.8% N_2

* Test 2 was later changed to 90% N_2-free + 10% O_2
The composition was then 28.9% O_2, 20.7% Ar, 50.4% CO_2

RESULTS

INTRODUCTION

The experimental results of this part of the study are presented in the following sections. Table 3 lists the various parameters for the different intake oxidants tested.

Engine Performance

The reduced power output for the nitrogen-free oxidizer compared to that for air was attributed to the delayed ignition. The large concentration of carbon dioxide delays the ignition by interfering with the chain propagating radicals that initiate the combustion process.

No attempt was made to adjust the injection timing to compensate for the increased ignition delay experienced with the nitrogen-free oxidizer. As a

Table 3. Engine Data

Parameter	Oxidizer 80.9% N_2 19.1% O_2	80.0% N_2 20.0% O_2	79.0% N_2 21.0% O_2	75.2% N_2 24.8% O_2	71.4% N_2 28.6% O_2	28.9% O_2 20.7% Ar 50.4% CO_2
NO (g/IkW-hr)	0.72	1.48	2.13	4.17	7.05	0
NO_x (g/IkW-hr)	1.03	1.93	2.73	5.27	8.06	0
CO(g/IkW-hr)	2.74	1.98	1.96	0.42	0.15	1.88
HC(g/IkW-hr)	2.78	1.65	1.85	0.56	0.23	0.72
Particulate (g/IkW-hr)	1.69	1.49	1.31	0.61	0.30	0.41
Extract (mg/IkW-hr)	86.5	49.6	44.6	51.7	57.7	14.2
SOF (%)	5.12	3.33	3.43	8.48	19.22	34.68
Fuel Rate (kg/hr)	0.96	0.95	0.95	0.95	0.96	1.0
BSFC (kg/IkW-hr)	0.37	0.37	0.39	0.38	0.38	0.47
Ignition Delay (^oCA)	20.7	20.0	19.6	18.6	17.9	24.5
Peak Pressure (Bar)	61.2	59.4	54.5	62.7	59.7	49.2
Exhaust (^oC) Temperature	444.4	472.2	491.1	493.3	470.0	587.2
Head (^oC) Temperature	168.3	175.6	182.8	184.4	186.7	196.1
Power (BkW)	2.58	2.54	2.42	2.53	2.53	2.14
Inlet (Bar) Pressure	1.07	1.04	1.01	1.04	1.07	1.01

result a large concentration of supplemental oxygen was required to start the engine and it fired several seconds after being motored at the operating speed. This permitted a large quantity of fuel to accumulate in the piston before violent ignition occurred. Two pistons and ring sets failed prior to developing a safe starting procedure.

Pressure traces for some of the different inlet oxidizers are shown in Figure 3, and peak pressures are listed in Table 3. Some of the traces in which the oxygen concentration is below 21% show high peak pressures. Since the fuel and oxidant have a longer time to mix and accumulate during the increased ignition-delay period, the combustion process approaches constant-volume combustion, and the resulting maximum pressures may be high.

Gas Phase Emissions

The gases which were analyzed in the exhaust are as follows: oxides of nitrogen, carbon monoxide, carbon dioxide, oxygen, and unburned hydrocarbons. The pollutants regulated by the U.S. Environmental Protection Agency are the oxides of nitrogen, carbon monoxide and unburned hydrocarbons. The data are presented on an indicated power-specific mass-flow basis (grams per indicated kilowatt-hour). This emission rate was chosen in order to standardize the mass of pollutant with respect to the power. Since this engine is small, a large portion of the fuel energy is used for frictional work. Indicated power was used to allow a closer correlation with other engines.

Carbon Monoxide and Unburned Hydrocarbons

Unburned hydrocarbon and carbon monoxide emissions are shown in Figure 4. These two pollutants result from incomplete combustion, and the trends were the same for each of them. As the oxygen concentration increases, the two pollutants decrease. Lean combustion accounts for this effect, since the oxygen-to-fuel ratio increases.

Figure 3. Pressure Traces

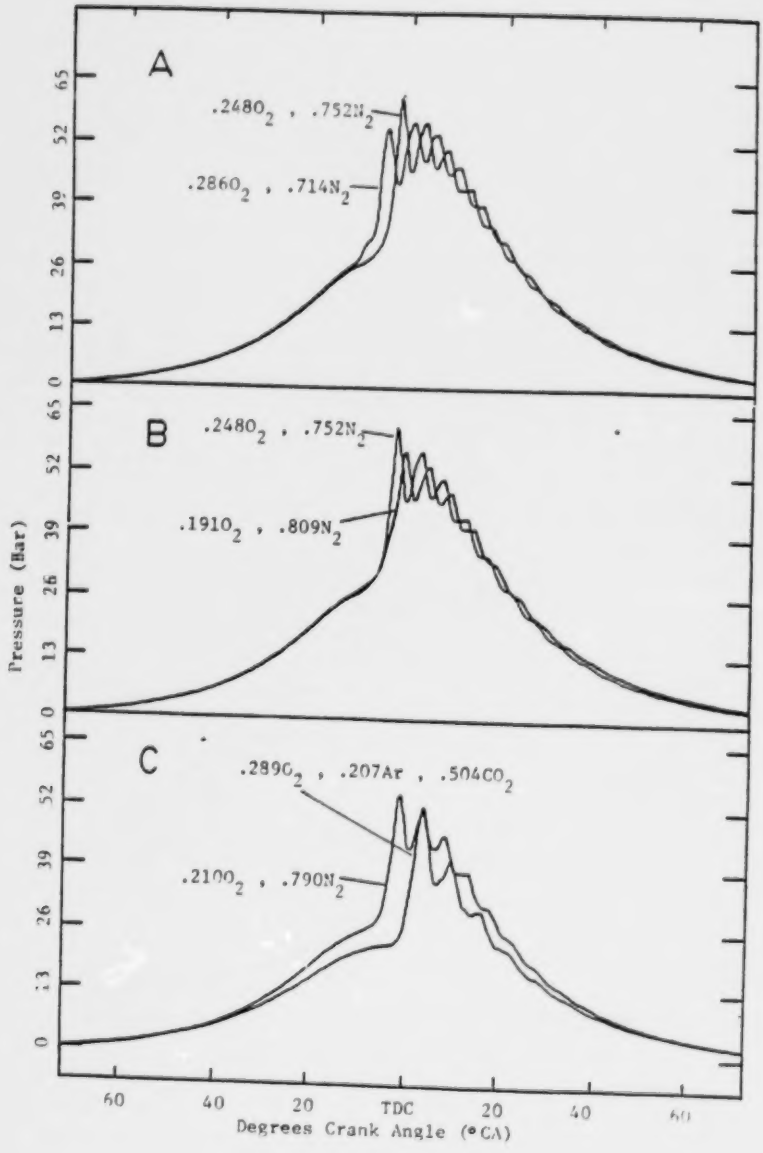

Figure 4. Carbon Monoxide and Unburnt Hydrocarbons as a function of Oxygen

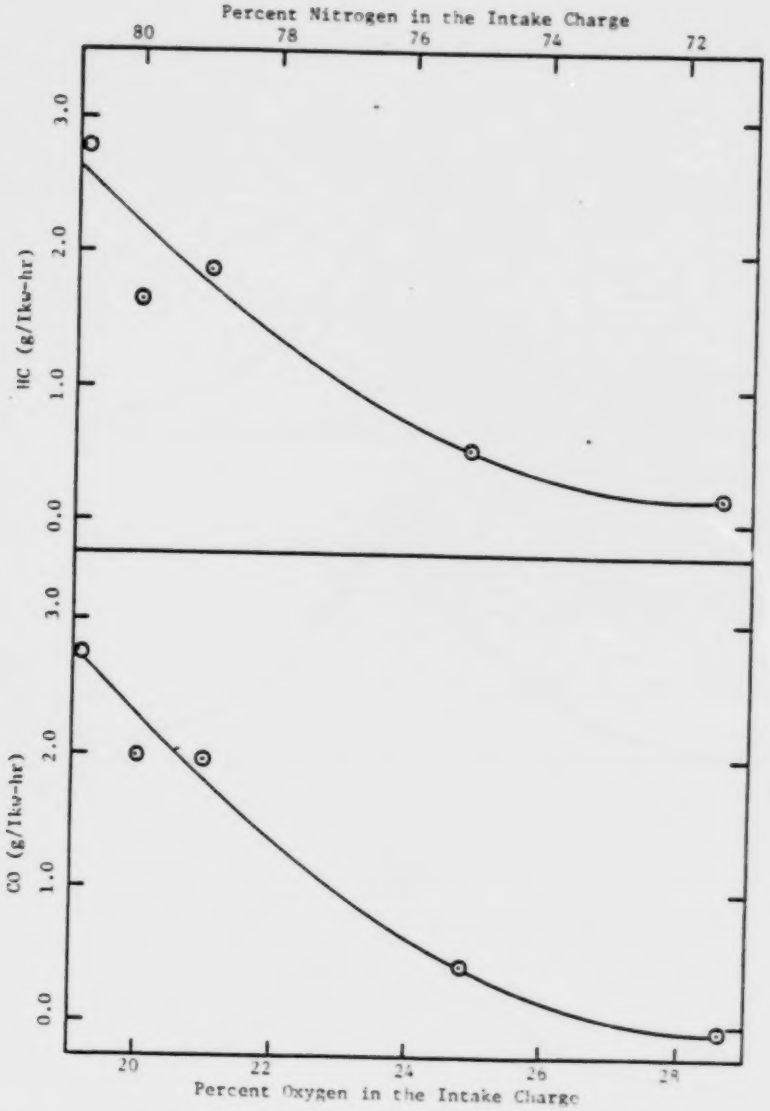

Oxides of Nitrogen

Figure 5 shows the trend in nitric oxide and nitrogen dioxide emissions with increasing oxygen concentrations. As the percentage of oxygen in the intake charge increases, nitric oxide increases linearly, and nitrogen dioxide reaches a maximum value near 25% oxygen. The Zeldovich mechanism as well as simple chemical kinetics predict these increases.

When excessive oxygen concentrations are used the combustion resembles a constant-pressure process and the resulting peak pressures and temperatures decrease so that the oxidation of nitrogen is discouraged. However, the high oxygen concentrations favor the oxidation of nitrogen since there is more oxygen available for the reaction. The result is two opposing phenomena. Since nitric oxide increases linearly with the oxygen concentrations the dominant factor in forming nitric oxide must be the oxygen concentration. It was found that nitrogen dioxide reaches a maximum value at the highest exhaust temperature and peak pressure. As the oxygen concentration further increases, the exhaust temperature and peak pressure decline and so does the nitrogen dioxide concentration. Thus, the temperature and pressure determine the formation of nitrogen dioxide at high oxygen concentrations.

Particulate Emissions

As the oxygen concentrations in the intake charge increase, the particle mass-emission-rate decreases sharply as shown in Figure 6. Since more oxygen is available to react with the carbon, fewer fuel-rich areas exist when the fuel is pyrolyzed. Also, the ignition delay is shortened by higher oxygen concentrations so that the fuel has more time to be oxidized and less time to pyrolyze.

The mass of organic adsorbate on the particulate matter was of concern because it contains biologically active compounds. The mass of the adsorbate increased with increasing oxygen in the intake charge. The large quantity of organic adsorbate that was extracted from the nitrogen-free particulate matter was formed from lubricant which was pumped into the upper cylinder during the long starting cycle.

Figure 5. Nitric oxide and Nitrogen dioxide as a function of Oxygen

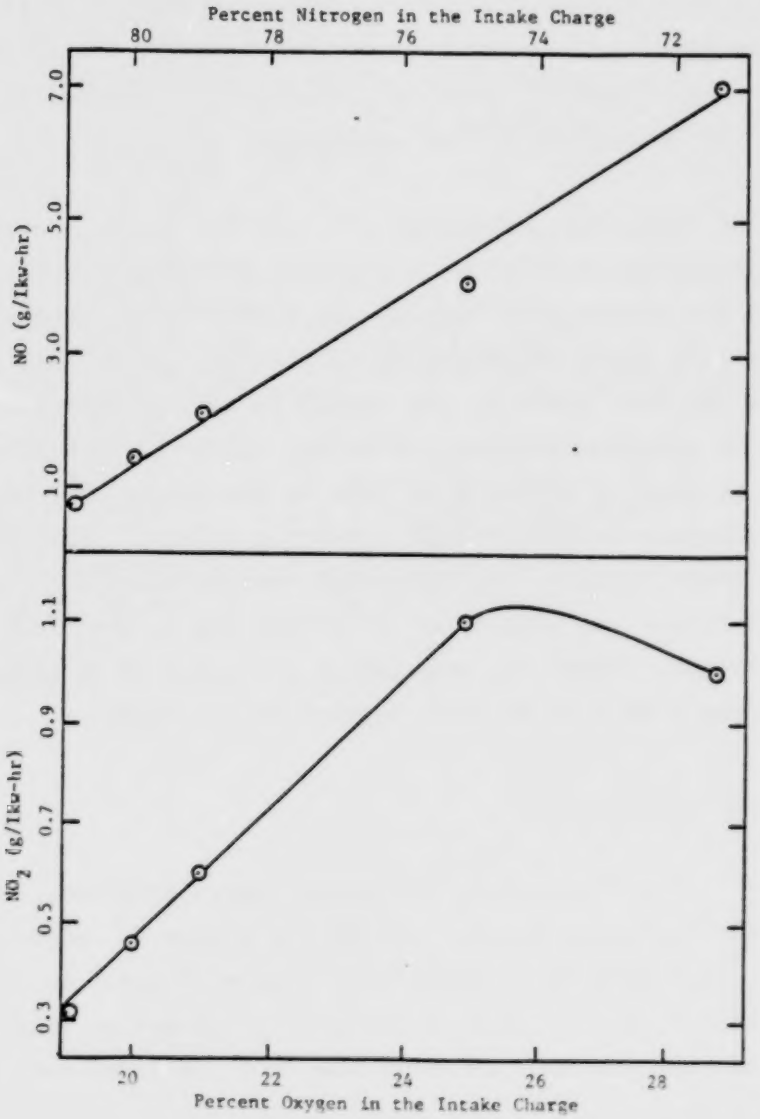

Figure 6. Ignition Delay, Particulate, and Extract as a function of Oxygen

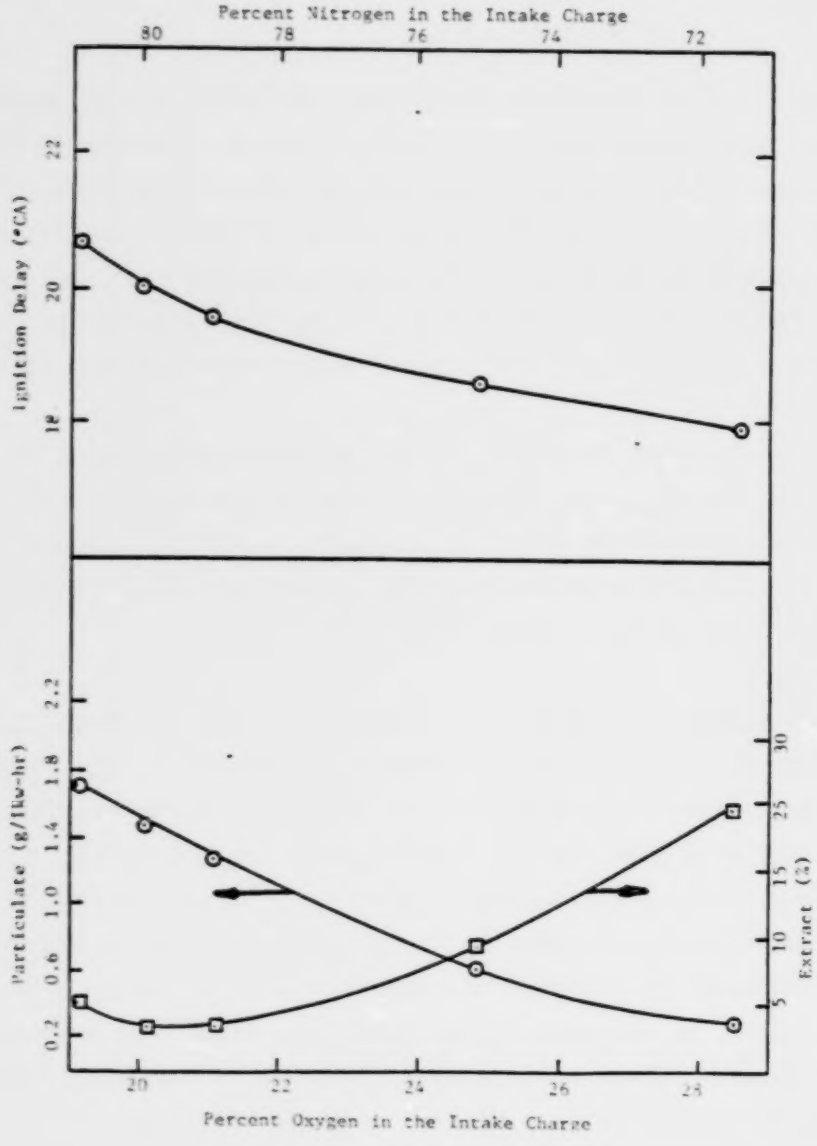

B. CHEMISTRY

1. CHEMICAL ANALYSIS OF ORGANIC ADSORBATES.

INTRODUCTION

Polynuclear aromatic compounds (PAC), and unburned fuel and lubricants constitute the major components of the soluble organic fraction of Diesel particulate matter. PAC include polynuclear aromatic hydrocarbons (PAH), as well as substituted and heterocyclic derivatives of PAH's. An understanding of the overall reactions leading to the formation of the PAC, and their environmental fate following release from the engine, is a requisite for a complete understanding of the health implications of Diesel engines.

The major objective of this part of the research was to provide a better understanding of the combustion process leading to the formation of the particle-adsorbed polynuclear aromatic compounds. Chemical characterization of the simplified soluble organic fraction, generated from a model aliphatic hydrocarbon fuel, was used to attain this goal.

Unlike the analysis of the soluble organic fraction generated from a full-boiling range fuel, the fuel simplifications introduced in this project have reduced the complexity to an extent that permits the separation and analysis of the entire SOF in a single pass. Capillary gas chromatography (GC^2) and high performance liquid chromatography (HPLC) were chosen as complementary separation techniques for the analyses. The effluent from the chromatographic columns were monitored by positive and negative chemical ionization mass spectrometry (CIMS), in addition to the standard detection methods for each separation technique. These methods have proven to be extremely useful for the separation and identification of trace organic mixtures.

EXPERIMENTAL

Capillary Gas Chromatography

Gas chromatographic separations were carried out on a Varian Aerograph Model 3700 Gas Chromatograph equipped with the requisite injector, detector and pneumatic options for capillary column operation. Separations utilizing flame ionization detection served as the basis for the subsequent GC^2/MS experiments, and the retention data were used for identifying the solutes. Nitrogen selective detection was employed for comparison of the nitrogen containing compounds from the air and the nitrogen-free oxidant.

The columns used in this study were 15μm or 30μm wall-coated open-tubular (WCOT) (0.9mm o.d. x 0.25 mm i.d.) borosilicate glass capillary columns, coated with a 30 μm film thickness of SE-54 stationary phase. The column was butt-end coupled to the injector insert with a 0.8 mm i.d. Vespel ferrule, providing a zero dead-volume fitting. Care was exercised to ensure that the column was cut at a 90° angle, and that pieces of septa were removed from the injector, in order to eliminate possible adsorption losses for higher boiling components of the samples.

The same flame tip was utilized for the flame ionization detector and thermionic specific detector experiments. However, the latter detector required changing the tower so that a ceramic-bead containing an alkaline earth salt could be positioned over the flame tip.

Ultra high purity nitrogen (99.999%) was initially used as the carrier gas to obtain adequate separations for the GC^2-FID and GC^2-TSD experiments, and as a charge-exchange gas for the GC^2/CIMS experiments. In subsequent studies high purity helium was used instead of nitrogen, in order to reduce analyses times. Injector and detector temperatures for all analyses were 270°C and 320°C, respectively. The column oven was temperature programmed from 100°C, with an initial hold of 1 min, to 300°C, with a final hold of 5 min. The temperature programming rate was 2°C/min for the helium

carrier gas. Injections of 1.0 μL aliquots of the samples were made, and the detector responses were recorded simultaneously on a strip-chart recorder and by computer data acquisition.

The computer used throughout these studies was a MODCOMP II/25 mini-computer, equipped with 64 kilo bytes of memory, direct memory processor, interval timer, three 1.3 mega byte moving-head disc drives, and a 9-track magnetic tape unit. Additional peripherals include a Tektronix Model 4662 digital plotter, Texas Instruments Omni 800 line printer, and Tektronix Model 1006 graphics display unit. The computer program gas chromatography (GASCHR) was used for the gas chromatographic analysis, and for the acquisition, manipulation, and presentation of the chromatographic data. Chromatographic data were stored on magnetic tape.

Capillary Gas Chromatography/Mass Spectrometry

Positive and negative ion chemical ionization mass spectrometry were used for the identification of the capillary gas chromatographic effluents and these results were confirmed by capillary gas chromatography/electron impact mass spectrometry.

The capillary gas chromatograph, which was used for the previous studies, was interfaced to a chemical ionization mass spectrometer via a heated fused silica interface. A Scientific Research Instruments Corporation BIOSPECT chemical ionization mass spectrometer was used for subsequent investigations. This system includes a chemical ionization source, quadrupole mass filter and a continuous dynode electron multiplier mounted off-axis to the quadrupole filter. The multiplier was modified to allow negative ion detection by grounding the entrance plate, and biasing the ion beam deflector so that it operated as a conversion dynode. In this manner, the multiplier could be operated with the same configuration in both positive and negative ion modes. The bias voltage used for negative ion detection was supplied by a Keithley Model 246 high voltage supply. The electrometer output was coupled to a Tektronix D10 single beam oscilloscope for real time display, and to a

computer interface for data acquisition. This study utilized the extensive computer software package, entitled program CAD, which was developed by our research group(12). The program is constructed in overlay format to conserve computer core, and allows for real time data acqusition and display of mass spectra, as well as manipulation, presentation, storage, and retrieval of collected data. Data for the GC^2/MS experiments were collected in the CRMS mode, in which the quadrupole mass filter is scanned at a software designated rate, with a chosen delay between each scan, and each mass spectrum is saved separately. The greatest number of mass spectra that can be accommodated by the disc storage with the present software system is 400 scans. Because capillary GC peaks are typically less than 10 sec in duration, and the chromatographic analysis takes at least 30 min, the limitation of 400 scans/experiment would seriously reduce the chromatographic resolution of the GC^2/CIMS experiments. A modification of the data acquisition overlay COLECT has alleviated this problem, by use of a threshold test. The operator specifies a threshold at the outset of each experiment, and only those mass spectral scans which contain at least one point whose intensity exceeds the threshold are saved. In this manner, only those scans which occur during the elution of a chromatographic peak should be saved. Appropriate modifications were made to the plotting, storage, and retrieval overlays to accommodate the data from the threshold experiments.

Identical chromatographic conditions for the GC^2/CIMS experiments were used in order that the data could be compared. The mass scale was calibrated with the ions from methane and methyl stearate. The collection of mass spectral data was initiated following elution of the solvent and restoration of the normal operating pressure (2×10^{-5} torr). Mass spectra were collected in the range from m/z 110 to m/z 310 at a rate of 75 scans/min for the duration of the chromatographic run, using an empirically derived threshold. The mass spectral data were stored on magnetic tape.

GC^2/EIMS data were obtained using a Finnigan Model OWA-20/30B GC^2/MS System and a Hewlett-Packard Model 5985 GC^2/MS System. Both systems were equipped with splitless injectors, and 30um fused-silica columns coated with

SE-54. Column effluents were directed into the MS source through fused-silica interfaces. Both mass spectrometers used quadrupole mass filters and the mass spectra were collected in the range 1 to 500 m/z. Associated computer hardware and software were used to acquire the data and to perform library searches based on the National Bureau of Standards library of 25,000 mass spectra.

High Performance Liquid Chroratography

During the initial stages of this research, soluble organic extract samples were separated using a solvent extraction scheme to remove the acidic and basic fractions from the neutral portion of the extract. The neutral fraction, which comprises greater than 90 percent of the mass of the extract, was separated by column chromatography on silica gel into paraffinic, aromatic, transitional and oxygenated fractions. Two difficulties which became apparent, were poor separation reproducibility and the requirement that the entire sample be used for the separation. Because the number of sample transfers was large, and the sample size typically less than 1 mg, contamination of the samples often resulted. As a result the impurities often dominated the subsequent mass spectrometric identifications. The fractions that were collected were characterized by chemical ionization mass spectrometry *via* a solids probe inlet. These early experiments indicated that the standard solids probe was unable to generate repeatable, rapid evolution of the samples. These difficulties led to the evaluation of HPLC methods for the separation of the extract, and prompted the development of a temperature-programmable, platinum-wire probe for the MS characterizations.

HPLC separations of the extract were accomplished using a gradient elution system, and UV absorption detection, followed by collection of the effluent for subsequent mass spectrometric identifications. A microprocessor-controlled Varian Model 5000 Liquid Chromatograph equipped with a 6-port Valco Model AH-60 sample injector and a 254 nm UV absorption detector, was used for the separations. The separation was performed on a 4.6 mm x 25 cm column, packed with 5 μm silica (Spherisorb-S5W) preceded by a 4 mm x 5 cm guard column, packed with HC Pellosil. All the solvents used in the HPLC separations were "Distilled in Glass".

The gradient program was initiated from the microprocessor following injection of 25 µL aliquots of the extract. Solvent flow rates were maintained at 1.0 mL/min. The initial mobile phase of 100% n-hexane was held for 10 min, followed by a linear introduction of dichloromethane over the next 10 min. The mobile phase was held for 10 min at 100% dichloromethane. Acetonitrile was then introduced over the next 5 min, and held at 100% for the remaining 5 min of the separation run. This 40 minute program was followed by a reverse gradient to 100% n-hexane, which was held for 30 min in order to condition the column before the next sample. Sample effluents were monitored with a 254 nm, fixed-wavelength UV absorption detector, and the signal was recorded on a strip-chart recorder. Sixteen fractions were collected manually during the course of each 40 min experiment and were allowed to evaporate overnight at room temperature in the dark.

Mass Spectral Analysis of HPLC Fractions

Positive and negative ion, chemical ionization mass spectrometry was used to identify the components contained in the collected fractions. It has been demonstrated by other workers that rapid heating of the sample in the source of the mass spectrometer favors evaporation over competitive decomposition reactions, and they have been able to obtain mass spectra of thermally labile species(13-15). In light of these findings, a platinum-wire probe was developed for the introduction and rapid evaporation of the sample.

This temperature-programmable probe is capable of scanning linearly a wide temperature range under computer control. The present design allows the temperature of the probe to be raised from source-block temperatures to 700°C, at rates of up to 500°C/sec. The temperature of the probe tip is increased step-wise and the mass spectral and temperature data are collected at each step. The probe consists of a 0.255 mm o.d. x 2 cm platinum wire attached to 1.5 mm o.d. nickel leads, which are fed through a modified 6 mm o.d. solids probe. The platinum filament serves as both a sample heater and as a platinum resistance thermometer, allowing accurate sample temperatures to be calculated.

Figure 7 is a block diagram of the electronics which enable the probe to be operated under on-line computer control. This controller provides accurate measurements of the voltage across the filament and the current through the filament, allowing the resistance to be calculated at each sampling point by the application of Ohm's law. The cross-sectional area of the platinum wire is known, and the temperature coefficient of resistivity and resistivity at $0^{o}C$ have been determined by other workers(16). Provided that the length of the filament is known, these data can be used to calculate the temperature of the filament at each step.

The length of the platinum filament is exceedingly difficult to measure mechanically, since it is dependent upon the point of contact with the nickel leads. The length was therefore calibrated by repeatedly scanning the input voltage from 0.000 V to 0.125 V, and measuring the current, while the probe tip was immersed in an ice bath. The thermal capacity of the ice bath was sufficient to maintain a constant temperature for the filament over the range of input voltages. Ohm's law was used to calculate the resistance at each point, and a linear least-squares fit of the calculated resistances yielded the resistance at $0^{o}C$. This was used, in conjunction with the resistivity at $0^{o}C$, to calculate the length of the wire. Calibration data were stored on magnetic tape. Overlays calibrate temperature probe (CTPROB) and manipulate temperature file (MTFILE) have been added to program CAD to accomplish these tasks. Overlay view temperature data (VTDATA) was also added for the presentation of temperature profiles and for the calculation of linear-least-squares slopes for the temperature data. The calibration was checked on a daily basis over a one month period and found to be constant.

Evaporated HPLC fractions were dissolved in 20 µL of dichloromethane, and a 5 µL aliquot placed upon the probe tip. The sample was allowed to air dry for 2 min before inserting the probe into the mass spectrometer inlet. Upon insertion, mass spectral scanning commenced from m/z 110 to m/z 310, and 75 scans were collected during a 1 min experiment. Mass spectral data were collected using program CAD. Modifications were made to overlay COLECT which allow the operator to input the starting voltage, and up to 5 linear ranges of

Figure 7. Block Diagram of Temperature - Programmable Platinum Wire Probe

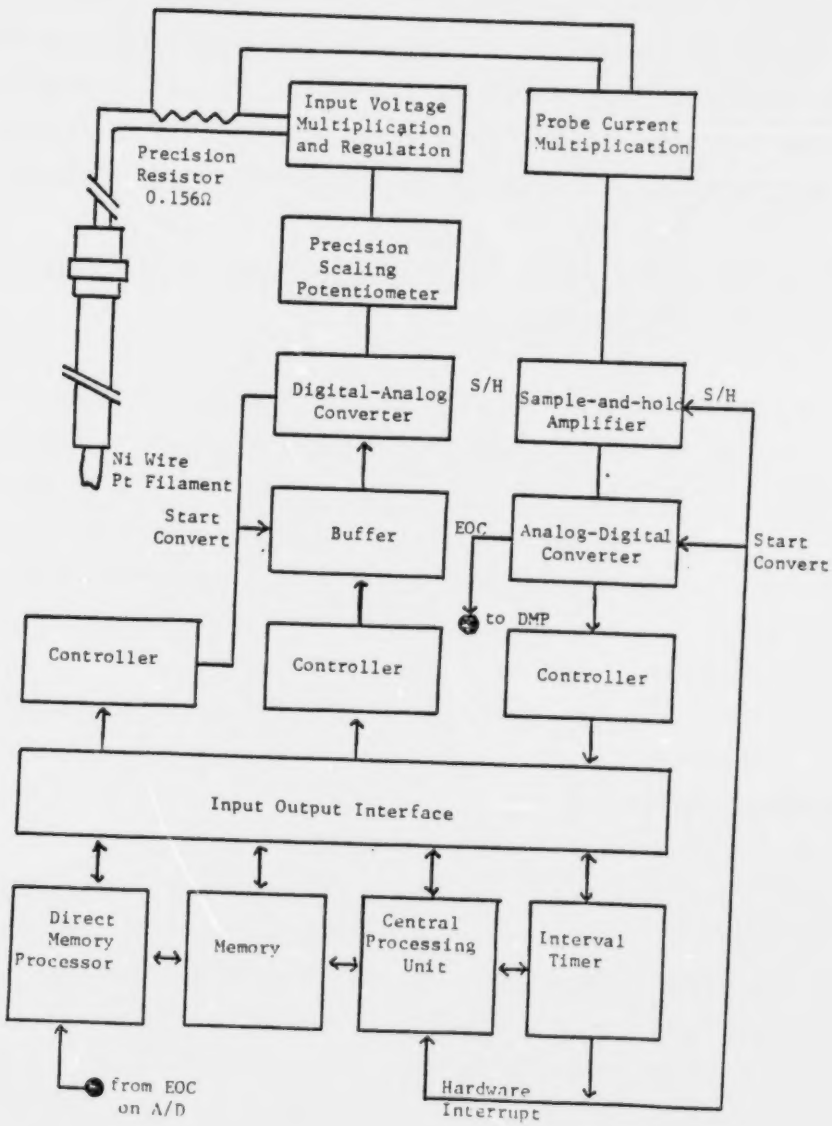

voltages for the platinum filament, for each experiment. The probe filament was maintained at 0.001 V for the first 10 scans in order to minimize evolution of the sample before the probe was seated in the source block. The voltage of the probe was then linearly increased from 0.001 V to 0.500 V over the remaining 65 scans. Since the source block was maintained at 150°C, a temperature ramp of 150°C to approximately 600°C was used in these experiments. This ramp allows the highly polar and involatile components of the samples to be rapidly vaporized, usually yielding intact molecular ions. Both positive and negative chemical ionization spectra were collected for each sample. The mass spectral and temperature data were stored on magnetic tape.

High performance Liquid Chromatographic Procedure for the Selective Determination of 1-Nitropyrene

A selective ultratrace analytical procedure which was developed by Dr. S. Tejada of the U.S. Environmental Protection Agency was used to quantify 1-nitropyrene(17). This procedure is based on isocratic reverse phase (water: methanol 80:20) high performance liquid chromatography with fluorescence detection (360 nm excitation, 430 nm emission). The essential feature of this method involved placing a reduction column (2 cm, platinum-rhodium catalyst on silica gel), maintained at 60-80°C, between two reverse phase octadecylsilane (ODS, 15 cm) columns. The first ODS column produced the initial separation and after 12 min the column effluent was passed onto the reduction column which reduced the nitro-aromatic compounds to amino-aromatics. The effluent from the reduction column passed onto the second ODS column. After 22 min. the reduction column and the first ODS column were switched out of the system and the separation was continued on the second ODS column. The 1-nitropyrene eluted after 27 min and was quantified by the fluorescence detector. After 45 min the entire system was programmed through a clean-up cycle.

RESULTS

Analysis of Organic Adsorbate by gas or liquid Chromatography - Mass Spectrometry

The extract from four air oxidizer and four nitrogen-free oxidizer collection runs were analyzed in these experiments. The gas chromatographic results, which were found to be the most sensitive means of fingerprinting the samples, demonstrated that there was excellent intrasample repeatability (correlation >0.95) and intersample similarity for the two sets of samples. These results show the reproducibility of the engine and fuel system used in this study.

Gas chromatographic retention data for the air oxidizer samples, based upon flame ionization detection results (Figure 8), and chromatographic data for standard compounds generated under the same conditions, were extremely useful for differentiating between various isomers of the polynuclear aromatic compounds. Retention indices presented in Table 4 were calculated using the system developed by Lee and coworkers(18). Peak areas were integrated after computer-assisted baseline subtraction had been performed. Average emissions presented in Table 4 in terms of ug/g particle and mg/kg fuel were calculated using a response factor for multiple injection of a standard solution of phenanthrene, calculated particle emission rates, and fuel consumption rates. Some of the minor peaks, which were not observed by capillary gas chromatography-electron impact mass spectrometry, could not be identified on the basis of their retention indices and their chemical ionization mass spectra. However, for completeness these compounds have been included in Table 4 with their nominal molecular ions.

The results for gas chromatographic separation of the nitrogen-free oxidizer samples, using flame ionization detection, are presented in Figure 9. The striking difference between these samples and the air oxidizer samples was the presence of relatively broad peaks throughout the chromatograms for

Figure 8. Capillary Gas Chromatogram of Air Oxidizer Sample using Flame Ionization Detection

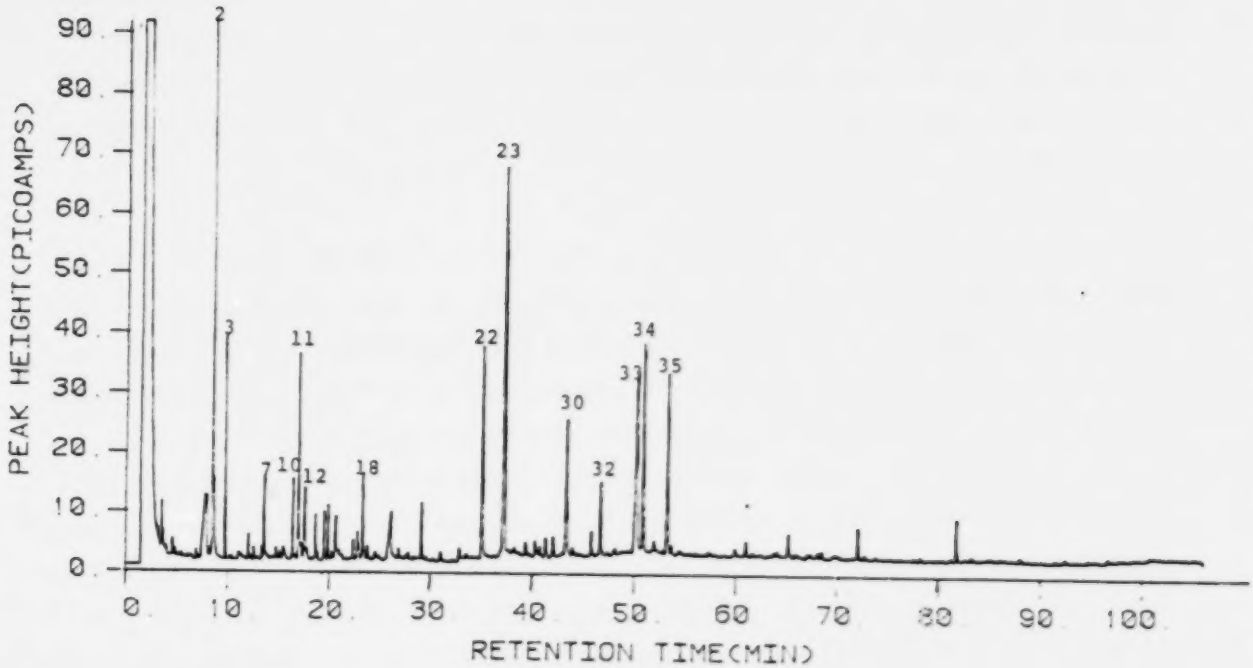

Peaks correspond to Table 4.

Figure 9. Capillary Gas Chromatogram of Nitrogen-free Oxidizer sample using Flame Ionization Detection

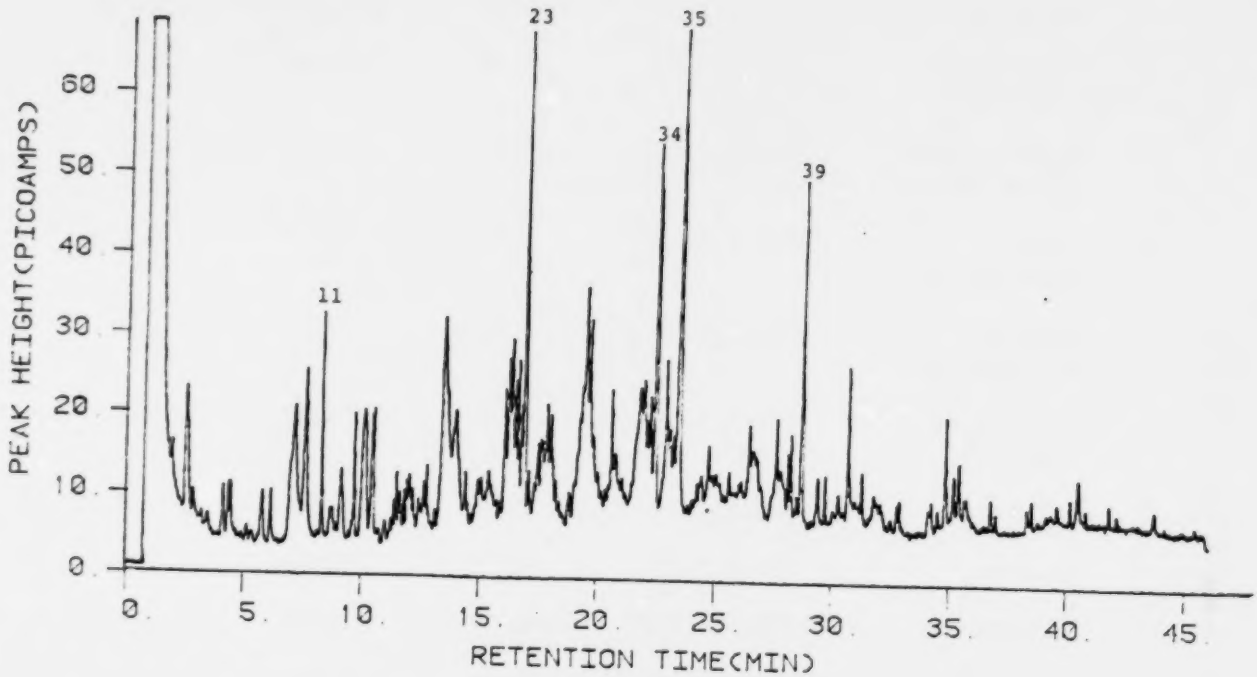

Peaks correspond to Table 4.

Table 4. Chemical Characterization of Organic Adsorbates on Diesel Particulate Matter

Ref. No.	Compound Name	Retention Indices M	Retention Indices SD	Average Emissions µg/g particle	Average Emissions mg/kg fuel	Method of Identification
1	Unknown	198.0	0.44	187.22	1.361	123-PCI
2	Naphthalene	200.0	0.10	329.10	2.394	a,b,d
3	Benzofuran, 7-methyl-	204.3	0.37	69.49	0.505	b,d
4	Inden-1-one, 2,3-dihydro-	212.3	0.19	22.41	0.163	b,d
5	Methyl-naphthalene	214.0	0.32	9.89	0.007	a,b,d
6	Methyl-naphthalene	216.6	0.51	11.12	0.081	a,b
7	Phthalate-anhydride	217.9	0.45	42.39	0.308	b,c
8	Unknown	222.0	0.56	12.66	0.092	147-PCI
9	Unknown	224.8	0.75	21.76	0.158	135-PCI
10	Biphenyl	227.7	0.76	76.38	0.555	a,b,d
11	n-Tetradecane	230.1	0.64	596.78	4.340	a,b,d
12	Unknown	232.1	0.87	83.04	0.604	147-PCI
13	Unknown	235.8	0.84	47.71	0.347	133-PCI
14	1-Benzopyran-2-one	238.7	0.91	42.77	0.311	b,c,d
15	Biphenylene, or Acenaphthylene	239.9	0.18	30.29	0.220	a,b,d
16	Acenaphthene	248.4	0.93	16.97	0.123	a,b
17	Unknown	250.0	0.94	27.70	0.201	197-PCI
18	Dibenzofuran	251.4	0.97	90.03	0.655	a,b,d
19	Unknown	253.4	0.99	20.20	0.147	157-PCI

Table 4. continued.

Ref. No.	Compound Name	Retention Indices M	SD	Average Emissions µg/g particle	mg/kg fuel	Method of Identification
20	Fluorene	266.6	0.55	21.46	0.156	a,b
21	Unknown	271.8	0.56	39.30	0.286	171-PCI,170-NCI
22	9-Fluorenone	292.6	0.21	232.03	1.688	a,b,c,d,e
23	Phenanthrene	300.0	0.11	582.44	4.236	a,b,d,e
24	Anthracene	301.6	0.19			a,b
25	Methyl 9-Fluorenone	306.7	0.16	29.58	0.215	c
26	Unknown	308.6	0.98	21.08	0.153	198-NCI
27	Methyl 9-Fluorenone	309.7	0.24	21.29	0.155	c
28	Unknown	311.0	0.26	15.13	0.110	198-NCI
29	Methyl 9-Fluorenone	312.8	0.10	20.35	0.148	c
30	Benzo[c]cinnoline	319.8	0.54	209.31	1.522	a,b,d,e
31	Fluorene Quinone	327.3	0.33	35.18	0.256	b,e
32	Phenanthrene Quinone	330.3	0.61	181.74	1.322	b,c,e
33	Cyclopenta-phenanthrene-5-one	341.7	0.82	501.67	3.649	b,c,e
34	Naphtho[1,8-cd] pyran-1,3-dione-, or Fluoranthrene	343.7	0.69	345.57	2.513	b,c,d,e a,b,e
35	Pyrene	351.4	0.97	309.75	2.253	a,b,d,e
36	Methylpyrene	365.9	0.21	8.82	0.064	a,b,e
37	Methylpyrene	372.9	0.25	6.04	0.044	a,b,e
38	Methylpyrene	375.8	0.92	22.21	0.162	a,b,e

Table 4. continued.

Ref. No.	Compound Name	Retention Indices M	Retention Indices SD	Average Emissions ug/g particle	Average Emissions mg/kg fuel	Method of Identification
39	Benzo[ghi] fluoranthene	389.4	1.13	64.08	0.466	a,b,d,e
40	Cyclopenteno[cd] pyrene	394.6	0.17	74.32	0.541	a,b,e
41	Chrysene	400.3	1.80	35.75	0.260	a,b,e
42	Benzofluor-anthene	436.1	3.55	16.75	0.122	a,b,e
43	Benzofluor-anthene	443.4	0.25	19.09	0.138	a,b,e
44	Benzo[ghi] perylene					e
45	Nitropyrene					e

a--Capillary gas chromatographic retention index
b--Gas chromatography/positive chemical ionization mass spectrometry
c--Gas chromatography/negative chemical ionization mass spectrometry
d--Gas chromatography/electron impact mass spectrometry
e--High performance liquid chromatography- Temperature-programmed chemical ionization mass spectrometry
Unknowns are identified by molecular ion observed either by positive (PCI) or negative (NCI) chemical ionization mass spectrometry.

the nitrogen-free oxidizer. These peaks are attributed to an increased level of lubricant in the combustion chamber, as a result of the start-up procedure for the modified oxidizer experiments. However, the major peaks in the nitrogen-free samples were the polynuclear aromatic compounds. These identifications were subsequently confirmed by gas chromatography-chemical ionization mass spectrometry.

When the flame ionization detector was replaced by a thermionic specific detector, which is a nitrogen selective detector, and the same samples analyzed, a lower number of nitrogen containing compounds were observed for the nitrogen-free samples compared to the air oxidant samples. This result is consistent with the reduction of the oxides of nitrogen in the exhaust, from an average of 470 ppm for the air oxidant to less than 1 ppm for the nitrogen-free oxidizer system. This indicates that the latter oxidizer system was successful in removing nitrogen from the combustion chamber. The low levels of nitrogen-containing compounds in all samples, in relation to the major components of the soluble organic fraction, precluded any positive identifications based on mass spectrometry.

Positive chemical ionization mass spectrometric total ion chromatograms showed a good correlation with the flame ionization results, and allowed the assignment of molecular weights for many of the solutes. With the exception of n-tetradecane, which showed a typical aliphatic hydrocarbon base peak at $(M-1)^+$, each peak exhibited a mass spectral base peak at $(M+1)^+$ resulting from proton transfer. Extracted ion profiling was used to deconvolute many of the minor peaks from the total ion chromatogram.

Negative chemical ionization mass spectrometry was especially useful as a selective tool for substantiating the presence of oxygenated derivatives of the polynuclear aromatic compounds, since the major non-oxygenated constituents of the samples did not produce ions. Base peaks in the mass spectra were observed at M^-, corresponding to resonance electron capture by the compounds containing the electronegative oxygen substituents.

Electron-impact mass spectra were used to confirm many of the identifications using searches of the National Bureau of Standards library of 25,000 mass spectra.

Liquid chromatographic separations of the same samples provided unique information, which was useful for the identifications, and Figure 10 shows a typical chromatogram. Fluoranthene, cyclopentaphenanthrene-5-one, and naptho[1,8-c,d]pyran-1,3-dione eluted in fractions 3, 8 and 14, respectively, while the gas chromatographic separation of the same compounds yielded retention indices which differed only by a single unit.

The temperature programmable solids probe developed in this study proved to be extremely useful for characterizing the involatile components of the soluble organic fraction. Many high molecular weight polynuclear aromatic compounds, including isomers of benzofluoranthene and benzoperylene, were identified by liquid chromatographic separation, followed by direct-probe chemical ionization mass spectrometry. These high molecular weight compounds were not eluted from the gas chromatographic column.

Nitropyrene was isolated and identified in fraction 6 of each of the air oxidant samples, and one of the argon/oxygen samples, using the temperature-programmable probe coupled with negative chemical ionization mass spectrometric detection. Concentrations were too low to quantify this compound in these experiments. The presence of this compound in one of the nitrogen-free samples is explained by the introduction of nitrogen into the combustion chamber as a result of cracking a piston ring during the experimental run. With this exception, the presence of nitropyrene only in the air oxidant samples indicates that its formation must occur as a secondary process, and is not dependent upon fuel-bound or lubricant-bound nitrogen.

The major compounds identified in the soluble organic fraction of Diesel particulate matter, generated from a two-component, aliphatic hydrocarbon fuel, are polynuclear aromatic compounds. The compounds identified are quite similar to those observed by investigators who employed full-boiling range Diesel fuels(19-21). These results indicate that the fuel used in this study is a good model of a full-boiling range fuel. The findings also imply that polynuclear aromatic compounds found on Diesel particles are inherent products of the diffusion-controlled combustion process, and are not only the result of

Figure 10. High Performance Liquid Chromatogram of Air Oxidizer Sample

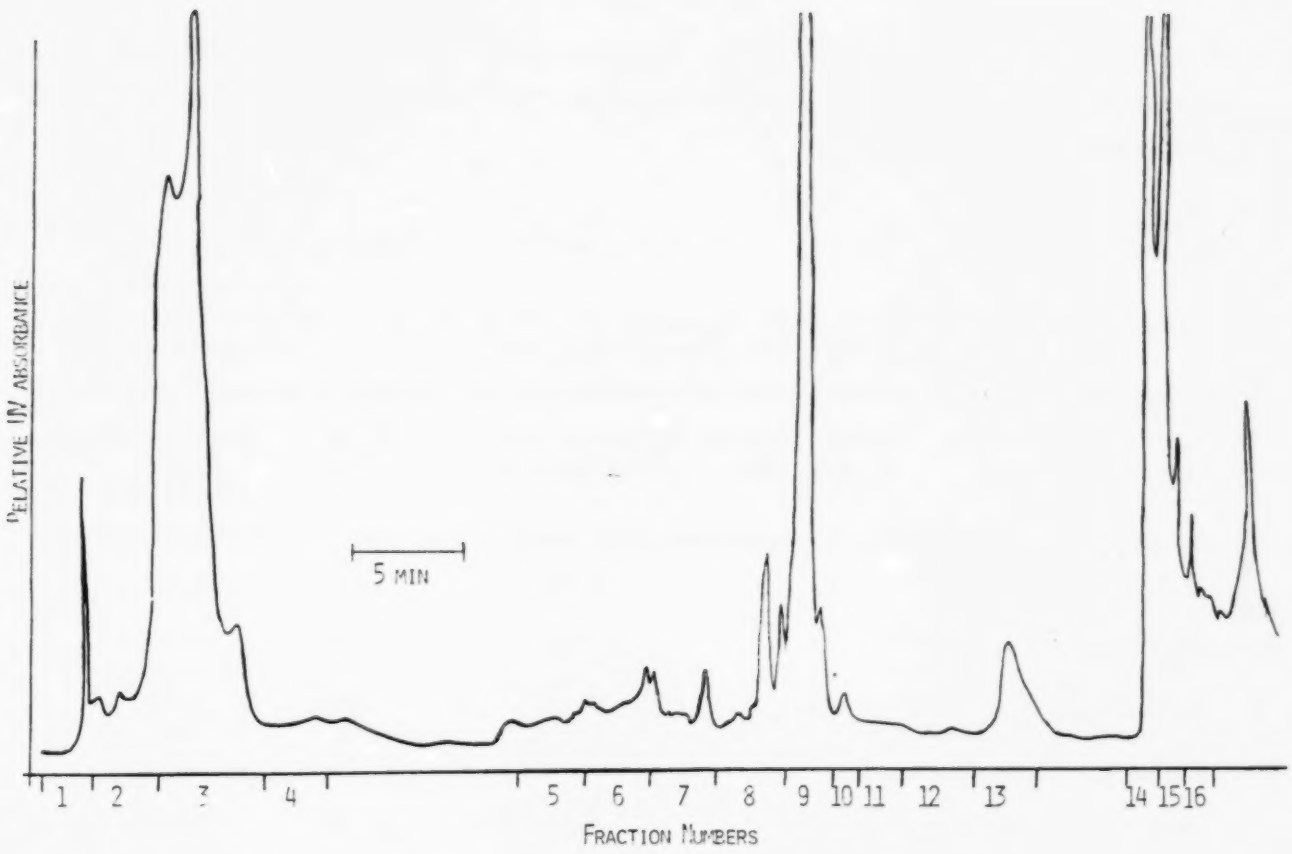

polynuclear aromatic compounds in the Diesel fuel persisting unchanged during combustion. In addition, the similarities between the compounds identified in this study and other investigations, where fuels included aromatic compounds, indicate that the polynuclear aromatic compounds must be formed from similar intermediates.

Selective determination of 1-nitropyrene

The extracts of the particulate samples, which were collected from engines operated on various oxidizers, were analyzed for 1-nitropyrene and the results are shown in Table 5.

Table 5. Concentration of 1-Nitropyrene in the Extracts of Particulate Matter Collected from Engines Operated on Various Oxidizers.

Oxidizer Composition (%)	1-Nitropyrene (µg/IkW-hr)	Nitrogen Dioxide (g/IkW-hr)	Pyrene (µg/IkW-hr)	Particulate Matter (g/IkW-hr)
19.1, O_2; 80.9, N_2.	42.1	0.31	ND	1.69
20.0, O_2; 80.0, N_2.	23.1	0.45	ND	1.49
21.0, O_2; 79.0, N_2.	4.6	0.60	406	1.31
24.8, O_2; 75.2, N_2.	32.5	1.10	ND	0.61
28.6, O_2; 71.4, N_2.	20.1	1.01	ND	0.30
50.4, CO_2; 28.9, O_2; 20.7, Ar.	0.3	0.0	120*	0.41

ND Not Determined;
* estimated emission rate, accurate quantification impossible due to the presence of lubricant in the sample.

These data are difficult to reconcile with our hypothesis that the emission rates of 1-nitropyrene follow the same trends as the emission rates of nitrogen dioxide. This hypothesis is based on reaction studies which will be discussed subsequently in this report. The data show that there are good correlations between the 1-nitropyrene and the particulate matter which suggests that these parameters are dependent. A possible explanation of this relationship is that the 1-nitropyrene is produced by reaction between the nitrogen dioxide and the pyrene sorbed on the particle. It may be that 1-nitropyrene is a sampling artifact i.e. it is produced by a reaction occurring during sampling. The nitrogen-free oxidant produces negligible quantities of 1-nitropyrene, which is consistent with levels of the nitrogen dioxide below the detection limit.

2. PHYSICOCHEMICAL PROPERTIES OF DIESEL PARTICULATE MATTER.

a. STATIC METHODS.

INTRODUCTION

In order to ascertain the relative extractabilities of compounds with potential adverse health effects, the physicochemical properties of the adsorbate/absorbent complex were determined. Although some preliminary work has been reported on the physical properties of Diesel particulate matter (22-24) there has been relatively little research into the thermodynamic properties of the adsorption process compared with numerous similar studies on carbon blacks (25-27) and coals (28). Physicochemical properties such as density, surface area, and heats of adsorption will to a great extent determine the nature of the sorbed compounds/particle surface system. Determination of such properties will provide a better understanding of the surface characteristics and potential environmental significance of airborne particulate matter.

EXPERIMENTAL

Samples

The carbon black used as a reference sample in these experiments was graphitized Spheron 6, a channel black that had been treated at 2700°C to give a highly uniform surface with an approximate B.E.T. nitrogen surface area of 80 m^2/g. Two Diesel particulate samples were used, the first DPM-PSU, was collected from the engine on the model fuel and the second Diesel sample, DPM-EPA, was collected from a 1978 Oldsmobile 350 engine by the U.S. Environmental Protection Agency (runs #8311-8319) operated with a commercial Diesel fuel and lubricant. This latter sample was collected after dilution.

Electron Microscopy

Electron micrographs were taken of the two Diesel samples with a JEOL transmission electron microscope at magnifications ranging from 10,000 to 50,000x. The microscope sample grids were prepared by suspending the particles in a 2% volume mixture of collodion and amyl acetate and coating this suspension onto copper mesh grids. Particle size measurements were made manually and the mean particle diameters were calculated from measurements of at least 100 particles using the following equation:

$$d_A = nd^3 / nd^2$$

where n is the number of particles counted with diameter, d. The external surface area was calculated by the following relation:

$$S_{ext} = 6/\rho d_A$$

assuming high and low densities, ρ, of 1.85 and 2.00 g/cm^3, after the method of Anderson and Emmett (29).

Densities and Adsorption Isotherms

A diagram of the apparatus used to measure helium densities and adsorption isotherms is shown in Figure 11. The capacitance manometer and associated electronics were obtained from MKS Instruments, Inc. The tubing and pressure sensor were maintained at temperatures higher than that of the sample cell so that the saturation vapor pressure was determined by the sample temperature.

Bulk densities of the solid samples were measured by weighing the quantity of particles occupying a known volume. True (or helium) densities were determined by expanding helium into the sample cell without and then with a known mass of particles.

Surface areas were calculated from adsorption isotherms with the method of Brunauer, Emmett, and Teller (B.E.T.) (30,31). The adsorbates used were nitrogen (16.2 $\mathring{A}^2$/molecule), benzene (40 $\mathring{A}^2$/molecule), and n-hexane (51 $\mathring{A}^2$/molecule) (32). The samples were degassed for 15-24 hours at the indicated "activation" temperatures (50°-400°C) in a vacuum of approximately 10^{-4} torr prior to each adsorption experiment to remove adsorbed materials from previous runs and to investigate the effect of varying the activation conditions on the available surface area. The gas buret was used to introduce increasing amounts of nitrogen and a 2.0 or 10.0 µL pressure-tight syringe was used to introduce the liquid organic adsorbates.

Heats of adsorption were calculated from two isotherms at two different temperatures using the Clausius-Clapeyron relationship. Adsorption heats were determined for benzene and n-hexane on several samples which had been heat-treated to varying degrees.

RESULTS

Electron Microscopy

The results of the electron microscopic measurements appear in Table 6. The average diameters of the DPM-EPA particles are less than that of DPM-PSU

Figure 11. Volumetric Adsorption Apparatus

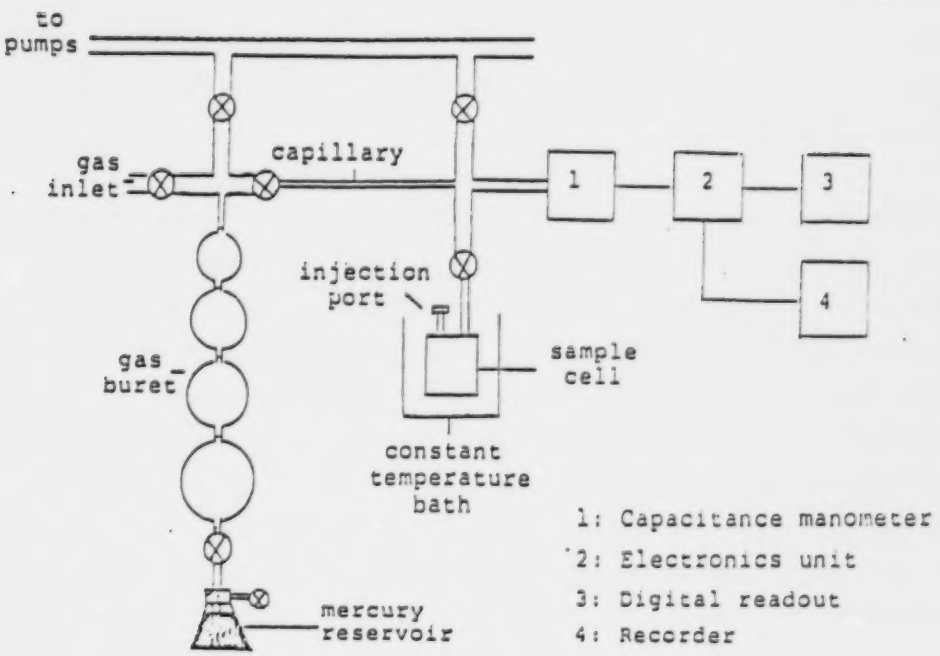

Table 6. Electron Microscopy Results.

Sample	Particle Diameter nm	Surface Area ρ=1.85	ρ=2.0
DPM-PSU	36	90.1	83.3
DPM-EPA	26.8	121.0	111.1
Grade 6 (29)	410	79.1	73.2

which is similar to that of a non-porous carbon black, Grade 6 (29). The external surface areas of the commercial Diesel samples are consequently greater. Particle diameters increase, and surface areas decrease, the greater the extent of graphitization of carbon blacks (22). However, external surface area can be deceiving if the solid is porous or heterogeneous. For this reason, external surface areas must be compared to adsorption surface areas (internal + external) to accurately characterize the surface.

Densities

The results of the bulk and helium density measurements are shown in Table 7. The bulk densities of the Spheron and of some suspended airborne particulate matter (33) are about 5 times greater than those of the Diesel samples. The true densities of all of the samples are similar because of the common carbon/hydrogen-based structure. The reported true density range for Spheron is that of amorphous carbon since it is 99% carbon (34). The helium density of DPM-PSU could not be accurately measured due to a small sample size, but the true density must be in the range of 1.5 to 2.0 g/cm^3 since it is 96% carbon (34). Bulk density will have the greatest significance with respect to atmospheric residence times. Particles which have low tendencies to agglomerate once emitted into the air and which have low bulk densities will remain in the air longer and can be transported longer distances than more dense aggregates of particles which will settle out of the atmosphere faster.

Table 7. True and Bulk Densities.

Sample	Bulk Density (g/cm^3)	True Density (g/cm^3)
Spheron 6	0.5	1.85-2.0
DMP-PSU	0.15	-
DPM-EPA	0.08	1.5-1.8
Atmospheric (33)	0.49-0.64	2.0-2.6
Diesel (23)	0.10	-

Adsorption Surface Areas

The measured BET adsorption surface areas are summarized in Table 8. The major sources of error were in the low pressure measurements and in the cumulative error associated with successive injected volumes. Consequently, the uncertainty in these values is approximately $\pm 5\%$.

The initial benzene adsorption on Spheron experiment yielded a surface area close to the assumed value of 80 m^2/g. The isotherm was S-shaped and of the Type II classification according to Brunauer, Deming, Deming, and Teller (35). This type of isotherm has a characteristic "knee" followed by an asymptotic rise to the saturation vapor pressure which is indicative of monolayer followed by multilayer formation. All isotherms measured for DPM-PSU were also of this type. An example of these isotherms is shown in Figure 12.

The adsorption of benzene on DPM-PSU after the initial nitrogen experiment resulted in a decrease in the surface area over three successive runs. The area was increased slightly with higher temperature activation but did not reach the initial area measured. This observation could be indicative of

Table 8. B.E.T. Surface Areas

Adsorbent	Activation Temperature (°C)	Adsorbate	Sample Temperature (°C)	Surface Area (m^2/g)
Spheron 6	400	Benzene	20-40	73.2
DPM-PSU	50	Nitrogen	-196	103.7
		Benzene	20	111.7
		Benzene	20	83.1
		Benzene	20-40	65.7
		Hexane	20	62.0
	100	Nitrogen	-196	77.7
		Benzene	-16-5	74.2
		Hexane	-21-0	77.5
	350	Nitrogen	-196	83.1
		Benzene	0-23	77.0
DPM-EPA	50	Nitrogen	-196	41.0
	200	Nitrogen	-196	69.7
		Benzene	0-20	65.3
		Hexane	0-20	74.5
	400	Nitrogen	-196	112.2
		Benzene	0-20	106.0

Figure 12. Adsorption Isotherms of Benzene on DPM-PSU (350°C)

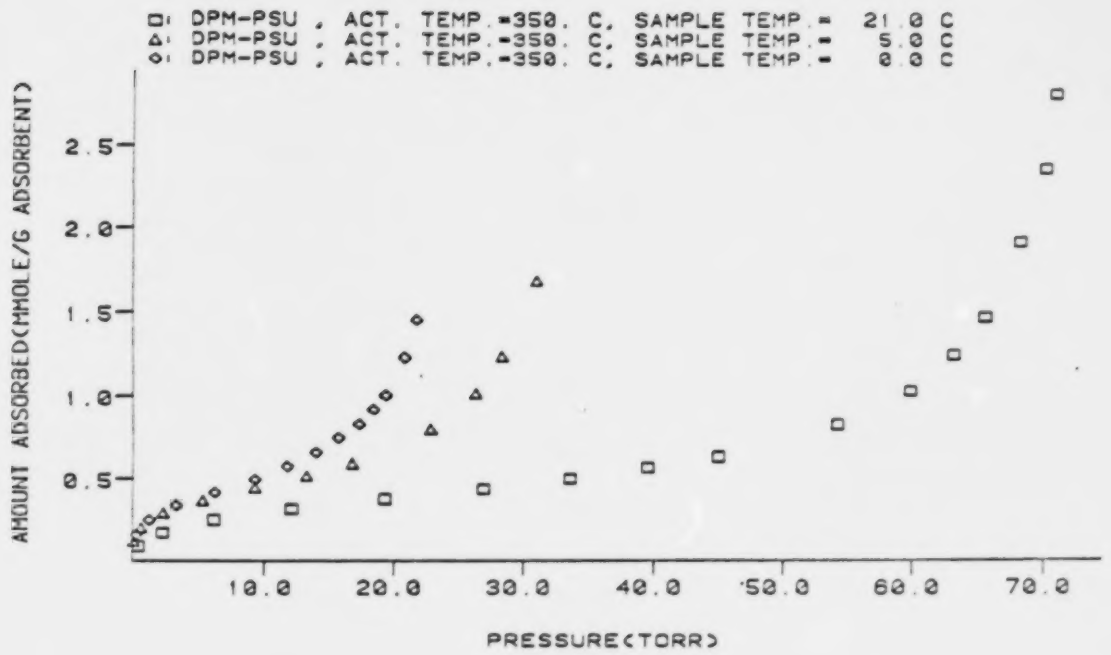

cracks or pores on the solid surface from which benzene could not be removed with the treatments employed here. The adsorption of benzene irreversibly modified the surface and the original nitrogen surface area should be taken as the actual surface area.

In contrast to DPM-PSU, the surface area of DPM-EPA was strongly dependent on the activation temperature. Multiple nitrogen adsorption isotherms for DPM-EPA activated to 50°, 200°, and 400°C are shown in Figure 13. The isotherm for the 50°C activation was calculated to have a BET C-value, a measure of the net heat of adsorption ($E_1 - E_L$), of 47, indicating a relatively low energy surface. The corresponding C-value for DPM-PSU was greater than 200. Increasing the activation temperature to 200°C resulted in a gain of approximately 30 m^2/g in area. Degassing DPM-EPA at 400°C increased the surface area to 112 m^2/g. The weight loss of this sample in the two high temperature outgassing treatments was approximately 17% of the original mass. It is reasonable to assume that the final outgassing effectively cleaned the surface of presorbed material since the weight loss due to these "thermal" extractions is close to the percentage extractable into dichloromethane, 17.5% (36). Since DPM-PSU was only 3% extractable into dichloromethane, it is understandable that degassing would have relatively little effect on the available surface area. The accessibility of more high-energy adsorption sites to nitrogen on the highly activated DPM-EPA is reflected in an increased C-value, 47 (50°C) to 300 (400°C), and BET surface area, 41 (50°C) to 112 (400°C). It seems likely that loss of presorbed material from cracks and narrow pores occurs in the high temperature activation and it is these newly unblocked sites that cause the increase in area and in energy of adsorption.

Benzene and hexane adsorption on DPM-EPA confirmed these changes in surface characteristics with increasing activation. Multiple benzene adsorption isotherms on DPM-EPA are shown in Figure 14. The "unactivated" sample, 50°C, yielded a Type III isotherm and a C-value between 1.5 and 2.5. In such situations, the benzene-benzene interactions are more significant than

Figure 13. Adsorption Isotherms of Nitrogen on DPM-EPA

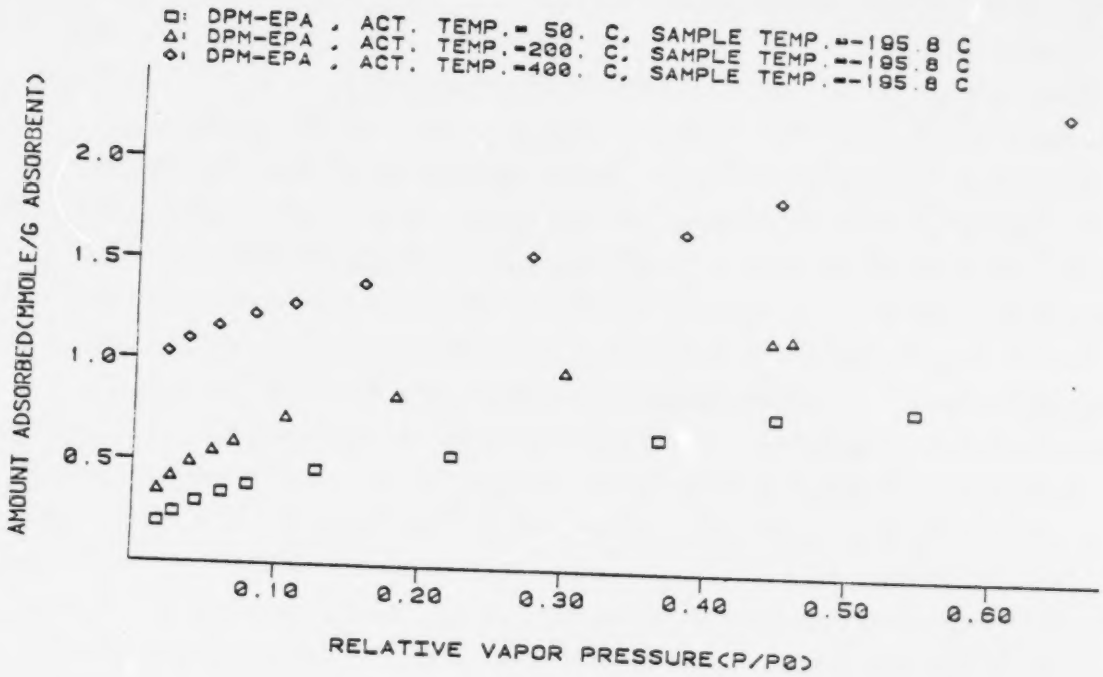

Figure 14. Adsorption Isotherms of Benzene on DPM-EPA

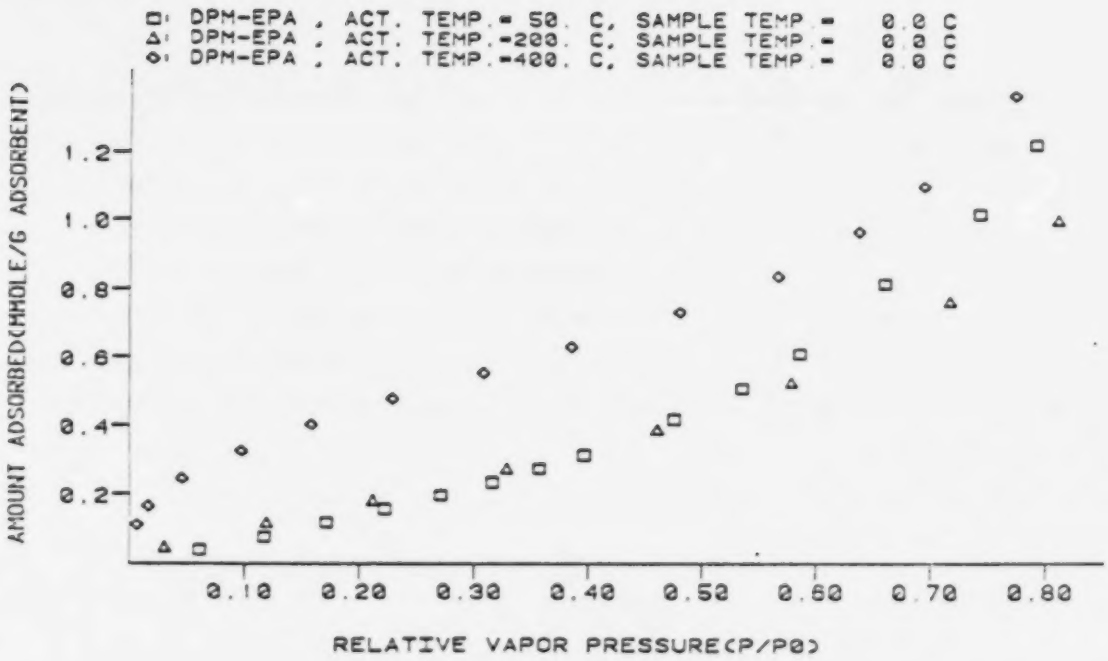

the benzene-surface interactions, and no distinct monolayer formation (knee) is observed in the isotherm. It is generally thought that the BET theory does not yield reliable surface areas in these systems (37,38).

The benzene isotherm for DPM-EPA activated to 200°C was Type II with a barely perceptible knee and an increased C-value of between 4 and 6. Consequently, these surface areas were close to those as measured with nitrogen. Adsorption on the highly activated sample yielded a Type II isotherm, also, with a C-value comparable to those of the DPM-PSU isotherms, 25 to 50.

The nitrogen BET adsorption surface areas and the external surface areas are compared in Table 9. The external areas are the averages of the ranges from Table 6. The roughness factor is the ratio of the BET area to the external area and is often taken as a measure of the porosity of a solid sample. The values for DPM-PSU in parentheses are those from the 350°C activation compared with those of the initial 50°C experiment. The roughness factors for both of the Diesel samples indicate little difference between the two surface areas. Both are less than the roughness factors for Grade 6, a nonporous rubber black, and Mogul, an ink black which is an example of a porous carbon black with a relatively large internal surface area.

Table 9. E.M. vs. B.E.T. Nitrogen Surface Areas

Sample	E.M. (External) Surface Area (m^2/g)	B.E.T. (Internal) Surface Area (m^2/g)	Roughness Factor
DPM-PSU	86.7	103.7 (83.1)	1.2 (0.96)
DPM-EPA	116.1	112.2	0.97
Grade 6 (29)	76.9	110	1.43
Mogul (29)	86.6	450	5.2

Heats of Adsorption

The variation of the heats of adsorption with surface coverage of benzene on Spheron is shown in Figure 15. The results are compared with those of Pierotti and Smallwood (39) and confirm the graphitic nature of the Spheron surface. The heats rise only slightly as the monolayer is formed and then at about 0.8 of one monolayer they decrease rapidly as second layer formation begins. The relative constancy of the heats while the first layer is completed is indicative of an energetically homogeneous surface.

The benzene and hexane heats of adsorption on DPM-PSU versus surface coverage are shown in Figures 16 and 17, respectively. The zero coverage isosteric heats, as determined by gas chromatography, have been included as well as literature data for graphitized carbon blacks (32,39). The initial benzene heats are much higher than those for the carbon black but the reverse is true for n-hexane (32). This is reasonable considering the surface groups (such as hydroxyls) on DPM-PSU to which benzene adsorption is sensitive and n-hexane is not (32). The other notable difference between the DPM-PSU and graphitized carbon black heats is the more gradual decrease in the heats past the maximum. Isirikyan and Kiselev (40) showed that the less homogeneous a surface is, i.e., lower graphitization temperature, the smoother is the heat curve and the higher is the initial heat. The benzene initial gas chromatographic heat is probably somewhat low, and is likely to be closer to 15 kcal/mole, considering the heterogeneity at low coverage and the affinity demonstrated by the decrease in the surface area. Although the inhomogeneity of the DPM-PSU surface caused high initial heats and a less rapid drop in the heats, the heat of adsorption curves, most notable for those for n-hexane, were not drastically different from those reported for some graphitized carbon blacks, especially those with residual heterogeneity (25).

The heat curves for benzene isotherms at 10° and 20°C on DPM-EPA activated to 50°C, are shown in Figure 18. The isotherms at this activation were Type III, indicative of adsorbate-adsorbate interactions being more significant than those between the adsorbate and the adsorbent. The high

Figure 15. Heat of Adsorption vs Surface Coverage for Benzene on Spheron 6

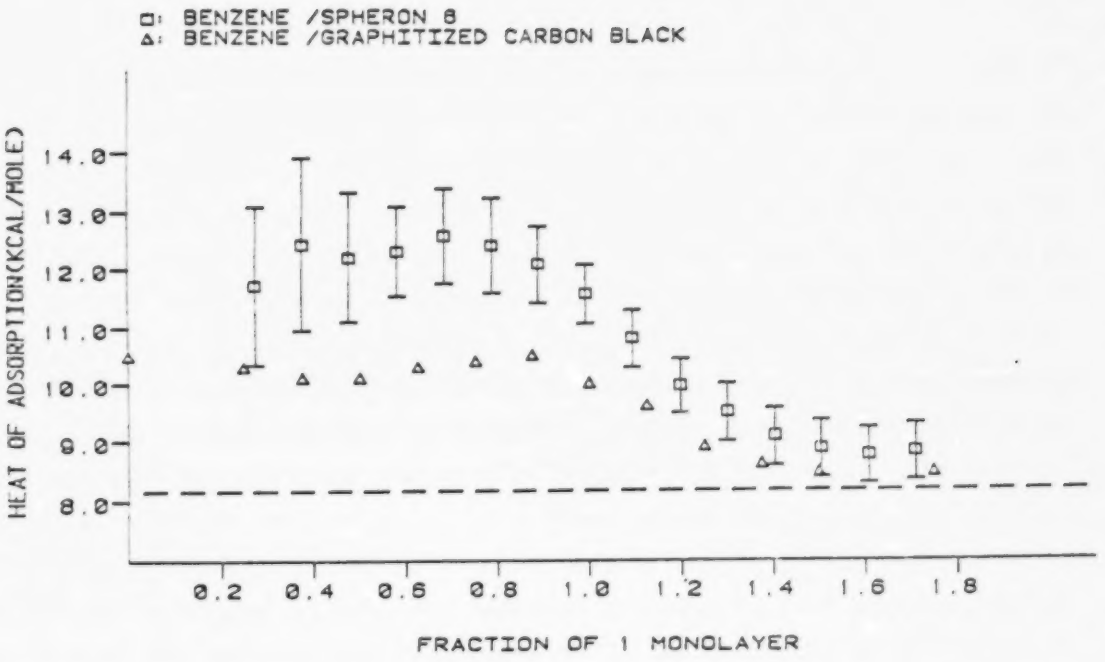

Figure 16. Heat of Adsorption vs Surface Coverage for Benzene on DPM-PSU (350°C)

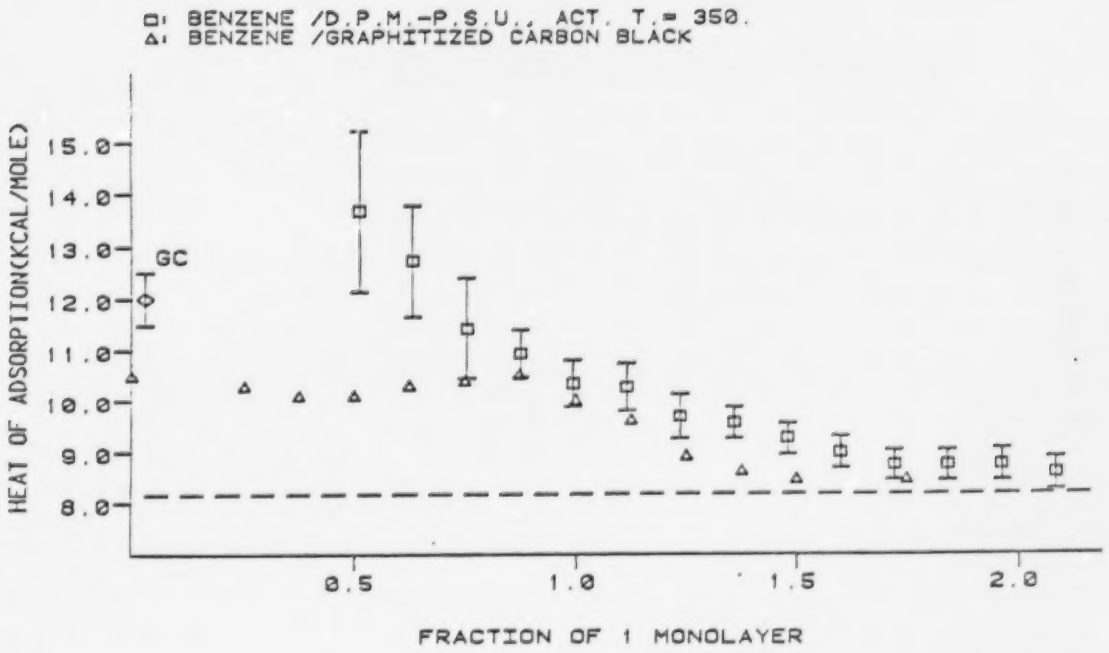

Figure 17. Heat of Adsorption vs Surface Coverage for n-Hexane on DPM-PSU (100°C)

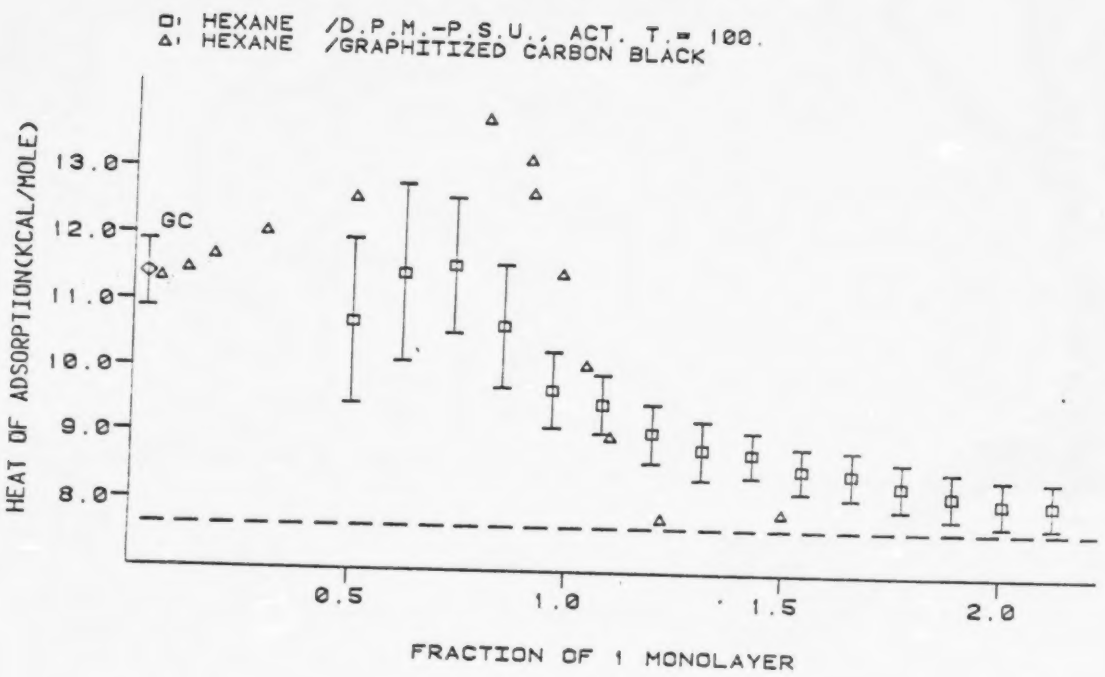

Figure 18. Heat of Adsorption vs Surface Coverage for High Temperature Benzene Adsorption on DPM-EPA (500C)

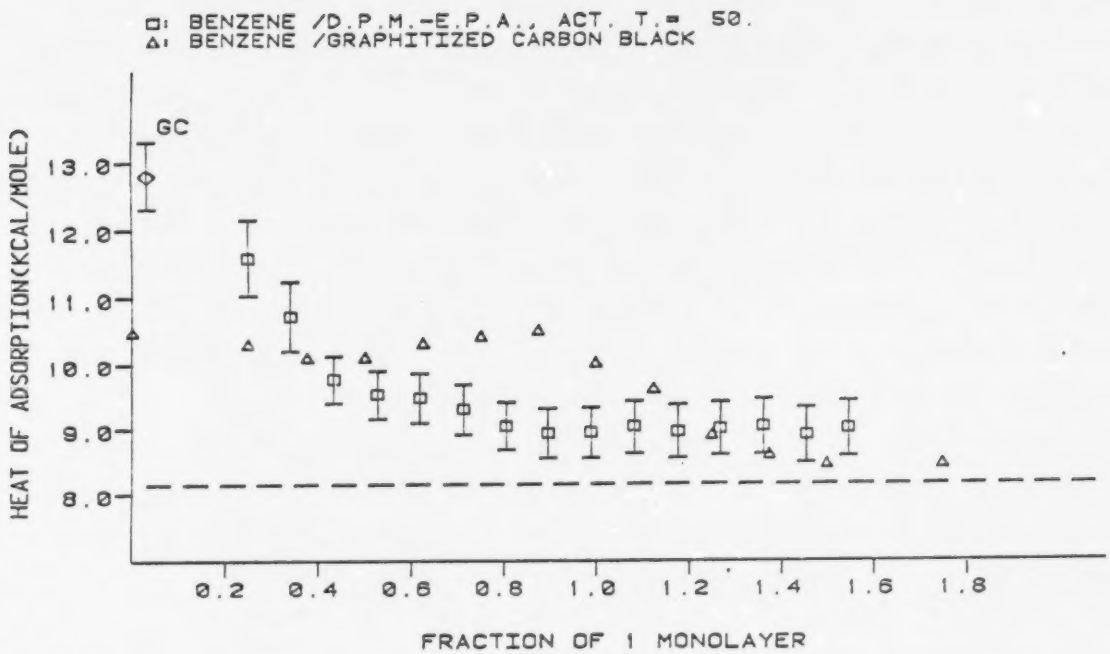

initial heats are due to the few high energy sites with which the adsorbate can interact. The heats fall very rapidly to the heat of vaporization well before monolayer coverage. The heat curve for benzene isotherms measured at 0^{o} and $5^{o}C$ on DPM-EPA, activated to $50^{o}C$, is shown in Figure 19. The initial heats are actually lower than the heat of vaporization of benzene, and then increase to that heat. This unusual dependence of adsorption heats on surface coverage is not unique. Babkin and Kiselev (41) demonstrated that benzene adsorption on a 100% methylated silica surface yielded similar heat curves. The process of replacing the hydroxyl groups with methyl groups resulted in changing the original high energy surface (Type II isotherm and high heats) to a relatively low energy surface (Type III isotherm and low heats). Thus, it appears that the heat curve obtained from the low temperature benzene isotherms corresponds to adsorption on a very low energy homogeneous surface due to the non-polar groups of presorbed molecules. Furthermore, the changes in apparent heat of adsorption with increased temperature are likely to be a result of changes in the nature (viscosity and surface tension) of the presorbed material. At higher temperatures, the adsorbate can more easily penetrate the film to reach the higher carbon adsorption sites, giving a heat that contains contributions from the heat of solution of benzene with the carbon substrate. The gas chromatographic heats were measured at temperatures greater than $50^{o}C$, which explains why those results fit on the higher temperature isotherm heat curves.

Incidentally, one can at least estimate the thickness of the layer of presorbed material of these samples by taking the volume per gram to be roughly the weight per gram (i.e., unit density) and dividing by the area of the layer. For the DPM-EPA this gives an estimate of 0.17 μL of preadsorbed material per gram of solid and, for an area of 41 m^2/g, an average preadsorbed layer thickness of 40 Å. (If such a layer were to liquefy, it is not unreasonable to suppose that benzene might dissolve in it with thermodynamic properties quite similar to those of a bulk solution).

Outgassing of DPM-EPA to $400^{o}C$ resulted in the heat curve shown in Figure 20. Removal of the presorbed material not only increased the available

Figure 19. Heat of Adsorption vs Surface Coverage for Low Temperature Benzene Adsorption on DPM-EPA (500C)

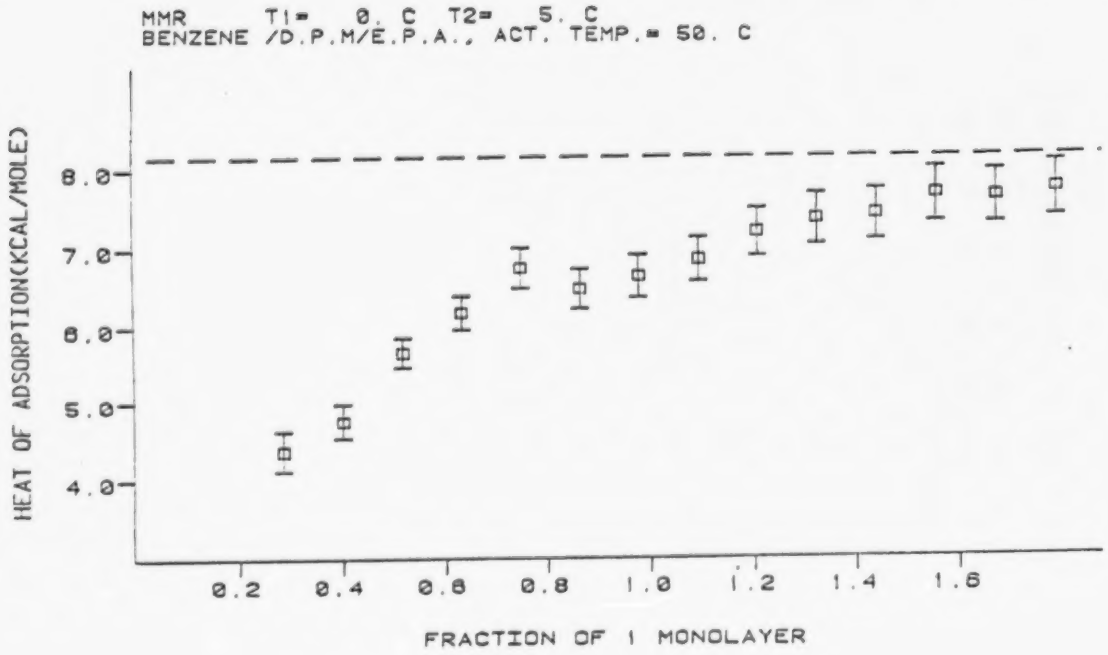

Figure 20. Heat of Adsorption vs Surface Coverage for Benzene on DPM-EPA (400°C)

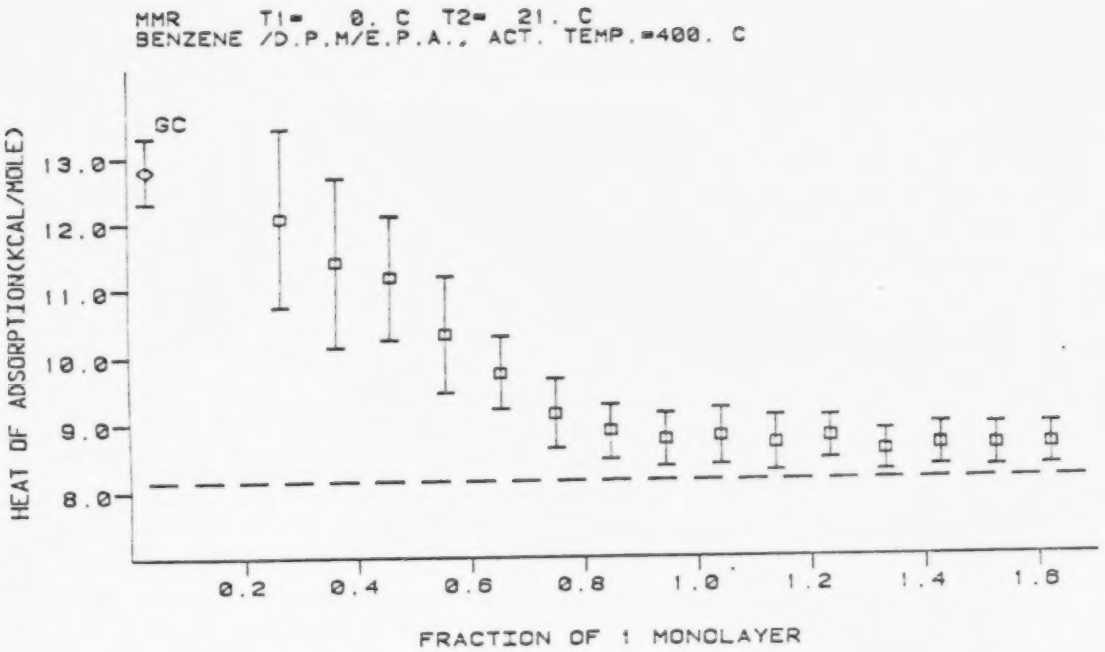

surface area but also gave higher heats of adsorption at higher surface coverages. For the 50°C activation (Figure 18), the heats in the 0.4 to 0.7 monolayer coverage range are 9.7 to 9.3 kcal/mole as compared to 11.4 to 9.4 kcal/mole for the 400°C activation. This is a result of increased exposure to carbon adsorption sites and a corresponding increase in the energy of the surface. It is interesting to note that the heats for benzene on DPM-PSU, activated to 350°C, in the 0.6 to 0.85 monolayer coverage range were 15.2 to 12.2 kcal/mole. Although high temperature activation of DPM-EPA increased the energy of the surface, the heats of adsorption of benzene on DPM-PSU remained higher. It is possible that further outgassing of DPM-EPA would bring the heat curve closer to that of DPM-PSU, but the presence of metals or other inorganic species may inhibit this.

b. DYNAMIC METHODS.

INTRODUCTION

Dynamic adsorption measurement techniques were also employed in order to compare these results with those obtained using the standard static method. The use of both measurement techniques enables the surface properties to be determined under widely different conditions.

One aspect of this study was treatment of particulate samples by heating and flushing with helium in the column and heating under vacuum prior to adsorption measurement. The effects of the variation of the injection volume on the measured adsorption heats were also determined. The heats of adsorption for some basic hydrocarbons on different carbon samples after various pretreatments should allow insight into the nature of the particulate surfaces and into the gas-solid interactions involved in the adsorption of vapors onto Diesel particulate matter.

The specific method used in this study has been reported previously by Ross, et al. (42). to measure the heats of adsorption for molecules on

graphitized carbon blacks. These workers showed that if adsorbate surface concentration tends to zero, then the following expression can be derived:

$$\frac{d(\ln t_r')}{d(1/Tc)} = \frac{q_{st}}{R}$$

where t_r' is the corrected retention time and Tc is the column temperature. Therefore, if a plot of log t_r' versus 1/Tc is made the resulting straight line has a slope equal to $q_{st}/2.303R$, (where q_{st} is the limiting isosteric heat of adsorption). This value of the heat of adsorption was found to be appropriate for the comparison with heats measured by the static method.

Since the flow rate changed from sample to sample as a result of differences in the packing densities of the adsorbents, the specific retention volume was used instead of the retention time. The specific retention volume was calculated using the following standard expression:

$$Vg = \frac{t_r' F}{m} \cdot \frac{Tc}{Tf} \cdot \frac{3}{2} \cdot \frac{\left((Pi/Po)^2 - 1 \right)}{\left((Pi/Po)^3 - 1 \right)}$$

where F is the flow rate, m is the mass of the adsorbent in the column, T_f is the temperature at the bubble flow meter, and Pi and Po are the pressures at the inlet and the outlet of the column.

EXPERIMENTAL

A gas chromatograph with a thermal conductivity detector (Varian 920) was used for all these studies; the glass column (2-mm i.d., 25-cm long) was packed with the adsorbents (Spheron 0.3g, DPM-PSU 0.1g, and DPM-EPA 0.06g). Helium (HP, Matheson) was used as the carrier gas with a flow rate in the range of 1.5 to 3 mL/min. The retention times of the various compounds were measured over a range of column temperatures (50-300°C) with the various adsorbents used in the previous studies.

In addition to measuring retention volumes of various compounds and using columns packed with raw Diesel particles, chromatographic data were also obtained after each of the following pretreatments: (1) 300°C with helium flow, in the column, for 15 hrs, and (2) 500°C under vacuum (10^{-2} torr) for 15 hrs followed by the first treatment.

The following compounds were used as the adsorbates: benzene, cyclohexene, cyclohexane, 1-hexene, n-hexane, methanol, n-octane, ethylbenzene, benzaldehyde, acetophenone, naphthalene, phenol, phenanthrene, fluorenone, fluoranthene and anthracene (all 99+% Aldrich reagents). The liquid compounds were introduced separately onto the column in a pulse size of 0.01-10.0 µL. The solid compounds were introduced in solution (25% in methylene chloride) in a pulse size of 1.0 µL. The column void volume was obtained from the air peak.

RESULTS

The specific retention volumes of each adsorbate on the various adsorbents were calculated from corrected retention times. These data were then plotted against column temperature to obtain the apparent heats of sorption or the isosteric heats of adsorption. Examples of these plots are shown in Figure 21. The major source of error in the determinations was the variation of the retention time. Consequently, the error associated with the heats is ±5%.

Isosteric Heat of Adsorption on Spheron 6

Preliminary experiments were performed with Spheron 6 to compare the values obtained for the isosteric heats of adsorption for benzene and n-hexane with those obtained by other workers using gas chromatography and similar adsorbents (43,44). Injection volumes (1.0 µL) of adsorbates, which correspond to <1% coverage of the available surface area of the adsorbent, were used since this coverage falls within the Henry's Law region of the adsorption isotherm (45). The chromatographic peaks obtained with Spheron 6

Figure 21. Gas Chromatographic Log Vr vs 1/Tc Plots for Benzene

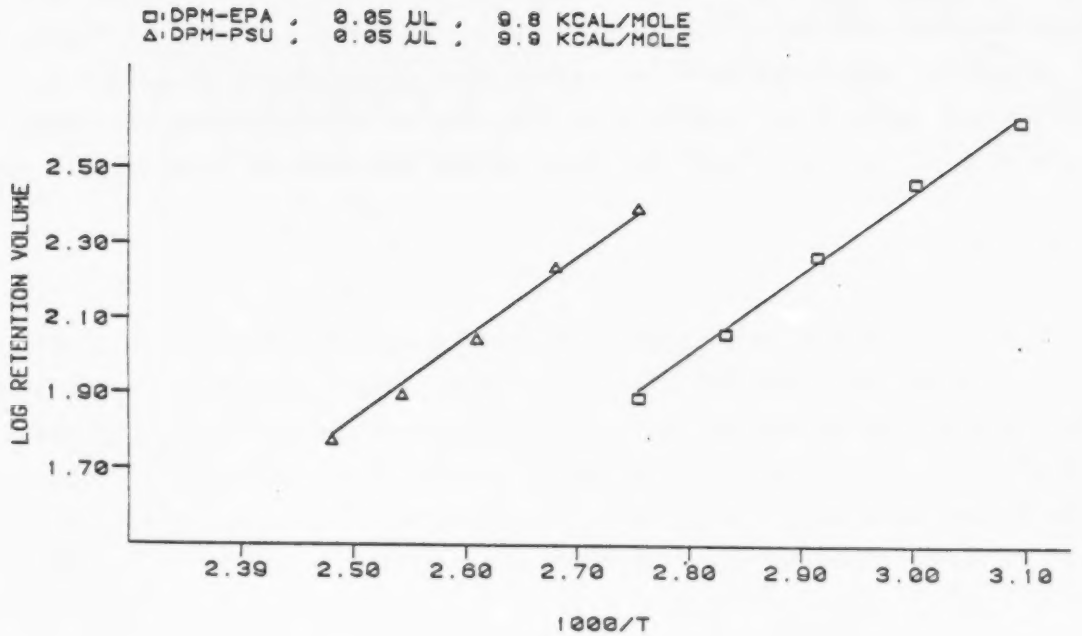

were sharp and symmetrical with very little tailing which is characteristic of a homogeneous and relatively non-porous surface. The values of the heats obtained in this study compared to the previous studies are shown in Table 10. The heats for the Spheron 6 are low compared with the heats on completely graphitized carbon blacks since graphitized Spheron 6 is known to have residual heterogeneity (i.e., it is not 100% C + H) in its surface.

Table 10 Isosteric Heats of Adsorption for Various Graphitized Carbon Blacks

Adsorbate	Isosteric Heats of Adsorption (kcal/Mole) Adsorbent		
	Spheron	Graphitized Carbon Blacks (43)	(44)
Benzene	8.7	9.4	9.8
n-Hexane	9.4	10.1	10.4

Pretreatment of Diesel Particulate Matter

The samples of Diesel particulate matter which were used in this and subsequent studies have significant quantities of sorbed materials on their surfaces (PSU 5% extractable (45) and EPA 18% extractable into dichloromethane (46)). These sorbed species will play significant roles in the surface properties of the particles. Therefore, the effects of various pretreatments were studied and the apparent heats of sorption of selected hydrocarbons were used to monitor these pretreatments. Unfortunately, the injection volume used (1.0 L) yielded heats of adsorption less than the adsorbate heat of vaporization. The adsorbate surface coverages were calculated (on the basis of BET surface areas of the adsorbents) to be quite high (40%) which must fall beyond the Henry's Law region of the isotherm. The heats measured,

therefore, have very little significance and are not reported here. However, since the DPM-EPA particles do have a larger quantity of presorbed material than the DPM-PSU particles, high temperature pretreatment should affect the adsorption heats on the former to a greater extent. This has been found to be the case with the static measurements discussed previously. The peak shapes for the adsorbates after all pretreatments were characteristic of heterogeneous, porous surfaces and Type II isotherm adsorbents (47). The presence of Type II isotherms was confirmed by the observation that as the injection volume was increased the retention volume decreased (23). The equilibrium constant decreases as the amount of the adsorbate increases and the isotherm is concave with respect to the pressure axis.

Effect of Surface Coverage on the Apparent Heats of Sorption

A Diesel particle is formed in the cylinder as a result of the combustion conditions present in the turbulent, heterogeneous flame. The particles once formed are transported from the cylinder to the ambient air in the exhaust gas which contains high concentrations of gas-phase species. Therefore, during the process of emission, the particles will be undergoing numerous collisions with the gas phase molecules and as a result the molecules will condense or adsorb onto the surface of the particle. The extent of condensation will be dependent upon the vapor pressure of the adsorbate and the temperature of the exhaust gases. Typical emission rates of particulate matter of 0.622g/mile have been observed by other workers (49) for light-duty automobile Diesel engines, of which 0.0715g/mile is extractable into organic solvents. Similarly, total hydrocarbon emission rates of 0.50g/mile have been observed with a hot flame ionization detector. If this hydrocarbon fraction is separated by gas chromatography, 50% of the total hydrocarbons have sufficient molecular weight to adsorb or condense on the particle. These figures suggest that approximately 28% of the available gas phase (hydrocarbons) adsorbs or condenses onto thesurface of the particles. The extent of the adsorption of the molecules will be related to the surface properties of the absorbent and the heat of adsorption of the adsorbate. However, once the particle has adsorbed moleculeson its surface, the heat of sorption of multilayers falls

below the heat of adsorption of the monolayer. The particles, which are collected on the filter, contain at least 18% by weight of organic extractable compounds indicating that the particles have multilayers of molecules sorbed on their surfaces. It is reasonable to expect that once the particle enters the ambient air it has sufficient sorbed molecules on its surface for its properties to be solely dependent upon the nature of the sorbed species.

Since the bioavailability of sorbed molecules is dependent upon the nature and the energy of sorption of the active species, a study was performed in which the apparent heat of sorption was measured as a function of concentrations of the adsorbate. The following adsorbates were investigated: acetophenone, benzaldehyde, benzene, cyclohexane, cyclohexene, ethylbenzene, n-hexane, 1-hexene, and n-octane. The adsorbents used in this study have been subjected to the highest temperature activation pretreatment. Table 11 lists some examples of the results of this study. These apparent heats of sorption suggest that the adsorbate first sorbs on the most energetic adsorption sites and then sorbs on sites with lower energies. The heats continue to decrease until there is a sufficient quantity of sorbed molecules on the surface that the energy of sorption equals the differential heat of evaporation from solution. Therefore, this study suggests that the history of collisions between the exhaust gases and the particle has a major effect on the energy of sorption.

Isosteric Heats of Adsorption for Diesel Particulate Matter

The small injection volumes (0.01 or 0.05 μL) used in the previous study correspond to coverage in the Henry's Law region of the adsorption isotherm and can therefore be used to quantify the isosteric heats of adsorption. Table 12 lists these heats for various adsorbates on the two samples of Diesel particulate matter activated at the highest temperature activation pretreatment. The higher molecular weight adsorbates phenanthrene, fluorenone, fluoranthene and anthracene could not be eluted from

Table 11. Variation Of Apparent Heats Of Sorption With Volume of Adsorbate Injected

Adsorbate	Adsorbent	Injection Volume (μL)	Apparent Heat of Sorption (kcal/Mole)
Benzene	DPM-EPA	0.01	12.8
		0.05	9.8
		0.10	9.1
		1.0	5.9
		10.0	8.7
	DPM-PSU	0.01	12.0
		0.05	9.9
		0.10	10.4
		1.0	7.6
		10.0	10.5
n-Hexane	DPM-EPA	0.01	15.0
		0.05	10.6
		0.1	10.4
		1.0	5.4
		10.0	12.8
	DPM-PSU	0.01	11.4
		0.05	11.4
		0.1	11.9
		1.0	8.4
		10.0	10.7

Table 12. Isosteric Heats of Adsorption

Adsorbate	Heat of Vaporization	Heat of Adsorption (kcal/mole) DPM-PSU	DPM-EPA	Graphitized Carbon Blacks (50)
Water	9.72	10.3	6.9	5.6
Methanol	8.98	9.0	4.8	5.3
Dichloromethance	-	8.6	5.0	-
n-Hexane	7.63	11.4	15.0	10.4
1-Hexene	7.79	10.6	10.2	-
Benzene	8.15	12.0	12.8	9.8
Cyclohexene	-	10.2	9.7	9.1
Cyclohexane	7.83	8.7	9.3	8.7
Ethylbenzene	9.3	15.2	8.3	12.7
Acetophenone	11.73	16.1	15.1	13.0
Benzaldehyde	11.66	17.4	12.2	-
n-Octane	9.2	15.2	8.4	13.4
Phenol	11.89	16.4	12.2	13.0
Naphthalene	12.31	16.4	12.3	17.3
Anthracene	16.82	-	11.1	-
Phenanthrene	14.18	-	19.0	-

the column containing DPM-PSU. These results can be rationalized on the grounds that the DPM-EPA sample is expected to have sorbed materials on its surface which cannot easily be desorbed. These materials will probably result from partially combusted lubricant (49).

The isosteric heats of adsorption determined for benzene and n-hexane on Spheron 6 are close to those reported in the literature for graphitized carbon blacks. The heats for the same two compounds on both Diesel samples are somewhat greater and this is probably due to the presence of higher energy adsorption sites on the heterogeneous porous Diesel particles. This heterogeniety is confirmed by the peak shapes and increasing retention volumes with decreasing injection volumes, indicative of a Type II adsorption isotherm. The difference between the isosteric heats of adsorption may be explained by the increased quantity of sorbed species on the DPM-EPA particle surface. Therefore, with the DPM-EPA samples, there is a higher probability of the adsorbate interacting with substances condensed on the particles than with the carbon particle itself. The variation of adsorption energies with injection volumes indicates a similar phenomenon. With increasing surface coverage, adsorbate molecules will be encountering fewer unoccupied adsorption sites and more adsorbed molecules. Multilayer adsorption will then occur and the corresponding interaction energies should be less. This has significance when considering the bioavailability of the sorbed species on inhaled particles. The molecules adsorbed on the high energy carbon sites will be tightly held as indicated by the isosteric heats, but additional layers of sorbed substances may be more easily liberated.

3. TRANSFORMATION OF DIESEL PARTICULATE MATTER.

INTRODUCTION

Particulate matter which is released into the ambient air is subject to various conditions including widely differing levels of gases and radiation. If the adsorbate-adsorbent system is reactive with respect to the prevailing atmospheric conditions, the compounds sorbed on the particles may be

different from those compounds identified in the organic extract of particulate matter collected in engine exhaust lines.

Electron paramagnetic resonance spectrometry (EPR) has been widely used to study the surface properties of carbon blacks (51-55) and coals (56,57). The EPR signal of carbon-based solids has been found to be dependent on numerous parameters including elemental composition and extent of graphitization. This aspect of the research describes the potential reactions that Diesel particulate matter may undergo with selected gases, and ultraviolet/visible radiation.

Electron Paramagnetic Resonance Spectrometry

EXPERIMENTAL

EPR spectra were obtained with a Varian E-104A EPR spectrometer using 2-milligram samples placed in quartz tubes. All experiments were run with a microwave power of 5 mW and a frequency of 9.515 GHz. The g-values were measured using α,α'-diphenyl-β-picrylhydrazyl (DPPH) as the external standard (g=2.0036) and the signal peak areas were measured with a planimeter.

Extracted particulate samples (-Ex) were prepared by 24-hour Soxhlet extraction of the particles with dichloromethane. Evacuated samples were prepared by degassing the particles at room temperature for one hour at a pressure of 10^{-4} torr. Heat-treated samples were prepared in the same manner but at a temperature of 150°C. The effects of the gases on the EPR signals were determined by allowing the evacuated samples to equilibrate for one hour with one torr of the gas prior to recording the spectrum. Irradiation experiments were performed in the EPR cavity using lens-colimated, filtered radiation from a 150 W high pressure Xenon arc lamp. The filters used were: 1. Corning #CS3-74 (low wavelength cutoff of 440 nm): and 2. Corning #CS0-56 (low wavelength cutoff of 240 nm). The signal maximum was monitored for 30 min with the lamp on, then for 30 min after the lamp was turned off.

RESULTS

The g-values and line widths of the heat-treated Diesel particulate samples are reported in Table 13. The relative positions of the EPR signals of DPM-EPA Spheron, and DPPH are shown in Figure 22. The reason for the displaced Spheron signal and the high g-value could not be ascertained. The g-values of the unextracted and extracted Diesel samples are close to the free electron g-value of 2.0023, and there was little variation from this value upon gas exposure or irradiation.

Table 13. Line Widths and g-Values

Sample	g(±0.0002)	Line Width(Gauss ±0.2)
DPM-PSU	2.0029	6.0
DPM-PSU-Ex	2.0028	8.5
DPM-EPA	2.0029	5.3
DPM-EPA-Ex	2.0030	7.0

However, the line widths of DPM-EPA and DPM-EPA-Ex are slightly less than those of the corresponding DPM-PSU samples. This could, in part, be due to the difference in the percentage of carbon, or the carbon-hydrogen ratio, between the two Diesel samples. In EPR studies of carbon blacks (51,55) with increasing graphitization the line width has been shown to remain essentially constant up to 90% carbon, and then decreases between 90-94% carbon due to exchange electron narrowing. The line width then increases above 94% carbon owing to the appearance of conduction electrons formed in the carbonization process. The difference in the line widths between DPM-PSU and DPM-EPA may also result from the presence of trace inorganic species in DPM-EPA, caused by the combustion of the numerous additives contained in the lubricant and commercial Diesel fuel (58,59). The synthetic lubricant and model fuel used eliminates the possibility of trace inorganic compounds on the DPM-PSU particles. The fact that the line widths of the extracted samples are greater

Figure 22. Relative Positions of EPR Signals

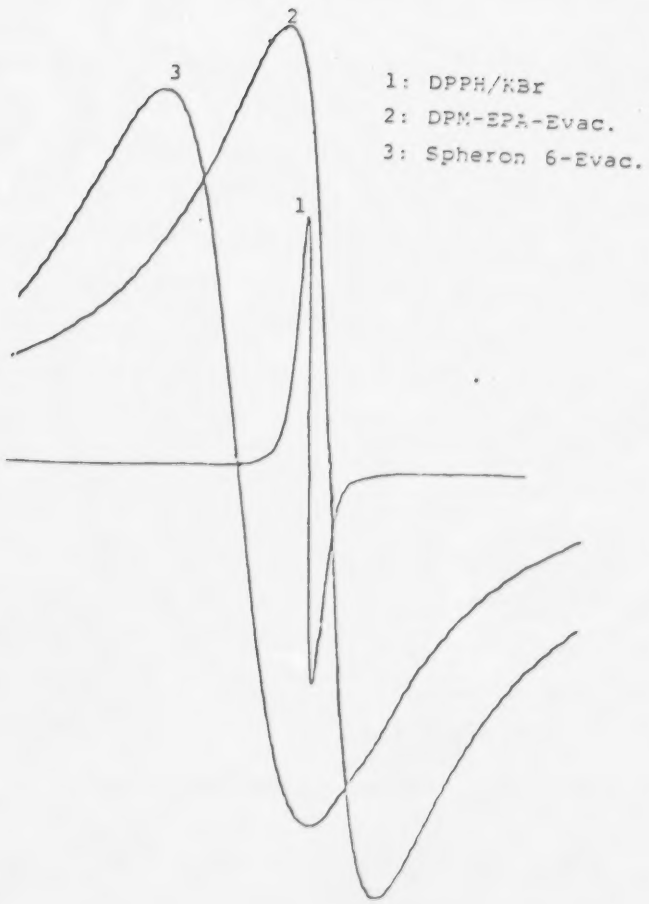

than those of the unextracted samples could be due to radical-radical broadening caused by the spin centers being closer to one another after the extraction process. The g-value and its fixed nature with respect to various treatments suggests that the EPR signal is similar to that for all carbon blacks. The variation of the line width between particulate samples raises the possibility of EPR being used to characterize particles emitted from different engines and to characterize the contributions due to different fuels and oils.

Although the EPR signal arises from the carbon-hydrogen substructure common to most carbon blacks, the signal can be affected by many surface treatments. Table 14 shows the changes in the line width and the integrated area of the signal for the DPM-PSU particles after a variety of pretreatments. Figure 23 shows the change in the actual DPM-PSU signal due to evacuation and subsequent heat-treatment. Similar effects were observed for DPM-EPA particles. Degassing the sample increases the signal intensity and narrows the line width, and heat treatment under vacuum increases this effect significantly. These observations probably reflect the removal of sorbed substances that physically interact with the radical centers and thereby broaden the signal. An evacuated sample could be exposed to the air, reevacuated, and the same signal characteristics retrieved suggesting the interactions affecting the signal were mostly physical in nature. By comparison of signal areas between known amounts of particles and DPPH, the spin concentrations were calculated. All were of the same order of magnitude, 10^{19} spins/g. This falls in the range of values given in the literature for carbon black spin concentrations (55).

Table 14. Effects of Various Treatments on the EPR Signal of DPM-PSU

Treatment	Line Width (Gauss)	Change in Signal Area
1 Atm. air	20 +/- 2	-
Evacuated	10 +/- 1	increase
Heat-treated	6 +/- 0.2	increase

Figure 23. Effects of Various Treatments on the EPR Signals of DPM-PSU

The effects of the selected gases on the signal of DPM-PSU-Evacuated are summarized in Table 15. The broadening of the signal, or "poisoning action", of paramagnetic gases such as oxygen and nitric oxide is well documented (51,52,55). Paramagnetic adsorbates cause line broadening by a primarily physical interaction between the gas molecules and spin centers of the solid. The spin-lattice relaxation time is decreased and the unpaired electron energy levels spread owing to the presence of the adsorbed species. However, this cannot explain the observed effect of the exposure of the particles to nitrogen dioxide. It has been shown by others (60) that the PAH, benzo(a)pyrene, adsorbed on filters reacts with nitrogen dioxide to form mutagenic nitro-derivatives. This suggests a possible mechanism by which additional radical centers could be formed upon exposure of the particles to nitrogen dioxide: the nitrated species react with phenolic or dihydroxy-compounds, which have been identified in the particulate extract

Also, hydrocarbons, which are present on the particles, are known to undergo hydrogen abstraction upon reaction with nitrogen dioxide (61);

$$R\text{-}H + NO_2 = R^{\cdot} + HONO$$

Either of these mechanisms could produce an increase in the radical concentration in the particulate matter. The technique of monitoring the EPR signal of the particles upon exposure to nitrogen dioxide proved to be a convenient method of following this interaction.

Table 15. Effects of Selected Gases on the EPR Signal of DPM-PSU

Gas (1 torr)	Change in Line Width (G)	Change in Signal Area
Oxygen	+ 3-4	-10%
Nitric Oxide	+ 2-3	-10%
Nitrogen dioxide	-	no immediate effect, +40-50% upon 24-hour exposure

Irradiation experiments were initially performed on the unevacuated samples to determine if the signal irradiation behavior was dependent on the wavelength of light used. The wavelength of irradiation was varied by the use of filters; a larger initial increase (6-8% of the original signal) with a slower subsequent decay of the signal intensity occurred as the wavelength was decreased to the ultraviolet region. The change in the signal was greater when more energetic radiation was allowed to pass to the sample. The effects of irradiation on the signal intensity of DPM-PSU with various treatments are shown in Table 16. Filter #CS3-74 was used in all of these experiments. The results were similar for DPM-EPA and the effects were less pronounced for the extracted samples. The irradiation effects on samples with oxygen or nitric oxide were similar to those of samples in air, although the net effect was an increase for the former, possibly because of low pressure. The greatest reactivity was observed for the degassed particles with no gases. The presence of air or low pressures of added gases decreased the interaction of the light with the radical centers. High temperature heat-treatment under vacuum or exposure of the samples to nitrogen dioxide had the common effect of inhibiting any net change in the signal intensity. It is interesting to note that even the extracted Diesel particles displayed significant sensitivity to irradiation while irradiation of Spheron 6 had no effect with any pretreatment. The radiation may ionize surface sorbed compounds, such as those with hydroxy groups, and cause them to lose electrons, thereby increasing the free radical concentration. The Spheron particles, lacking such adsorbed species, would not be expected to react to the light in the same way as the

Diesel samples. The sensitivity seemed to be the most pronounced when no interfering gases were present, in vacuum, and was greater the more energetic the radiation. When air or other gases are present the potential for photochemical reactions is increased. Characterization of these interactions would require much more research. These preliminary results indicate that Diesel particulate matter is sensitive to light although the exact nature of the interaction is not yet known. Thorough investigation of the photochemical reactivity of these particles would be worthwhile; there is presently a lack of information in this area. Knowledge of the effects of atmospheric conditions on potential biologically-active compounds sorbed onto the particles will yield a better understanding of the ultimate health risks posed by airborne particulate matter.

Table 16. Effects of Irradiation on the EPR Signal of DPM-PSU

Treatment	Light On	Light Off	Net Change
1 Atm. air	sharp increase slow decay level off	sharp decrease slow decay level off	decrease 5-10%
Evacuated	sharp decrease rapid increase level off	sharp increase slow increase level off	increase 30-50%
Evacuated + O_2 or NO	sharp increase level off	sharp decrease level off	slight increase
Evacuated + NO_2	sharp decrease level off	sharp increase level off	none

Formation Of 1-Nitropyrene By Reaction Of Nitrogen Dioxide With Diesel Particulate Matter.

EXPERIMENTAL

The EPR studies have demonstrated that Diesel particulate matter will react with nitrogen dioxide; this is a potential route for the formation of 1-nitropyrene. Therefore a study was undertaken in which the particulate matter collected from the nitrogen-free oxidant experiments was reacted with known concentration of nitrogen dioxide in the presence of water vapor at 52°C (the sampling temperature). The nitration system is shown in Figure 24. By varying the flow of the nitrogen dioxide (960 ppm) and high purity nitrogen, any concentration of nitrogen dioxide, which is monitored both before and after the filter, is possible. Using this system, nitrogen dioxide adsorption may be measured with a resolution of 1 ppm of nitrogen dioxide (62). To obtain a trace quantity of nitric acid, the nitrogen was bubbled through water. The particles were subsequently extracted and the 1-nitropyrene determined by the HPLC procedure already described.

RESULTS

The results of this study are shown in Table 17.

Figure 24. Nitration System

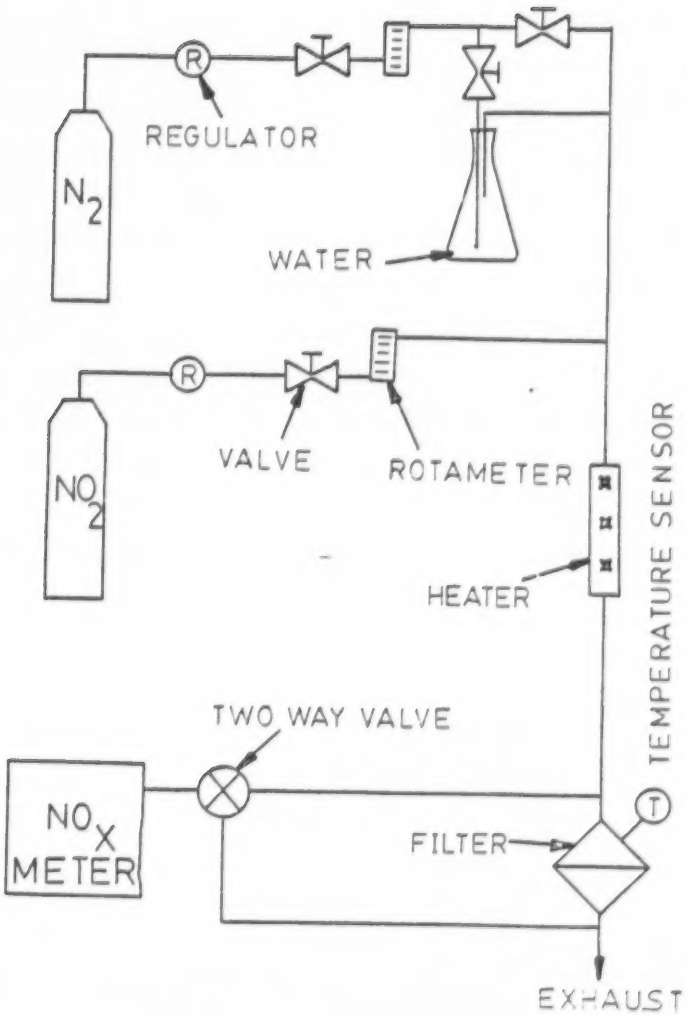

Table 17. Reaction of Nitrogen Dioxide with Nitrogen-free Particulate Matter.

Nitrogen Dioxide Concentration (ppm)	1-Nitropyrene Concentration (ppm)
0	2.0
5	44.6
50	76.6
100	221
150	248

These results suggest that 1-nitropyrene may result from the process of collecting the Diesel particulate matter since nitrogen dioxide (nitric acid) is present in the exhaust gas since the nitration can occur under typical sampling conditions. Also it is reasonable to expect that other adsorbates could be similarly nitrated.

C. BIOLOGY

INTRODUCTION

Two microbial assays were used in this study to measure the potential activity of Diesel particulate matter: the Ames test and the Comp test.

AMES MUTAGENICITY TEST

EXPERIMENTAL

Bacterial Strains and Media

The Ames mutagenicity test system requires the use of genetically constructed mutants of Salmonella typhimurium. The strains have been selected for sensitivity and specificity for reversion from histidine auxotrophy to prototrophy. There are several bacterial tester strains containing different mutations which render the bacteria auxotrophic for histidine. These strains contain unique types of DNA damage in the gene(s)

coding for the enzymes essential for histidine synthesis. In this study, TA1535, TA1537, TA1538, TA98 and TA100 were utilized, as recommended for routine Ames mutagenicity assays (63,64,65). A description of the genotypes of the various strains is presented in Table 18. TA1535 and TA100 have base pair substitutions in histidine synthesizing genes and can be used to detect mutagens causing base pair substitutions. Strains TA1537, TA1538, and TA98 contain frameshift mutations and are used to detect various frameshift mutagens. In addition to the histidine mutation, each tester strain contains two additional mutations: (1) the loss of the DNA excision repair capacity, and (2) the loss of the lipopolysaccharide (LPS) barrier that coats the bacterium. The tester strains TA98 and TA100 were developed by transferring a resistant transfer factor (R factor) to the standard tester strains TA1535 and TA1538, respectively (63,66). The presence of this factor makes the strains more sensitive to polycyclic hydrocarbons. All of the Salmonella strains utilized were obtained from Dr. Bruce N. Ames, Department of Biochemistry, University of California, Berkeley, California. Upon receiving the tester strains, frozen permanent cultures were maintained (63). In order to ensure that the bacteria used in the Ames test system had the correct reversion specificity, cultures of the various strains were routinely checked to confirm the required genotype (63-65). All five strains were checked for histidine and biotin auxotrophy, the presence of a "rough" outer envelope (rfa), the absence of inducible excision repair (uvrB), and the characteristic spontaneous reversion rate (per 10^8 cells) (63). In

Table 18. Genotype of the TA Strains used for Mutagen Testing

Histidine Mutation				Additional Mutations	
hisG46	hisC3076	hisD3052	LPS	Repair+	R factor
TA1535*	TA1537	TA1538	rfa	uvrB	---
TA100		TA98	rfa	uvrB	+R

*All strains were originally derived from S. typhimurium LT_2.

+ The deletion (Δ) through uvrB also includes the nitrate reductase (chl) and biotin (bio) genes.

addition, strains TA98 and TA100 were tested for the presence of plasmid pKM101 which conveys ampicillin resistance. Master plate cultures used for the inoculation of the nutrient broth cultures required in the test were prepared and maintained for no longer than one month (63). Overnight cultures (12hrs.-16hrs.) of the strains to be used in testing were grown in nutrient broth (Oxoid Nutrient Broth Media, #2) (63). The mutagenicity assay was performed on Spizizen minimal medium supplemented with 0.5% glucose (67). Top agar containing trace amounts of biotin and histidine was prepared (63).

Quantitative Ames Mutagenicity Test

The experimental procedure for the Quantitiative Ames Salmonella mutagenicity Test was performed in the following manner (63). 0.1 mL of a 12 to 16-hour nutrient broth culture of the tester strain (10^8 cells) was added to 2.0 mL of sterile top agar (0.6% Difco agar, 0.5% NaCl) (63). The top agar contains trace amounts of histidine and biotin (0.045 mM histidine-HCl, and 0.045 mM biotin) which allows all the bacteria on the plate to undergo several divisions; this growth is necessary in many instances for the expression of mutagenic events. Following the addition of bacteria, various concentrations of the sample to be tested were added (usually 0.1 mL or less), followed by 0.5 mL of S-9 microsomal mix (if required) (63). The contents were mixed and poured onto minimal glucose agar plates. The plates were inverted and incubated in the dark at 37°C for 48 hours. Following incubation, the numbers of colonies (revertants to histidine prototrophy) were determined using an Artek 880 automatic colony counter. In studies where unextracted particle samples were tested directly, the colonies appearing on the plate were counted by hand. Control plates without mutagen or S-9 mix were prepared in the same manner. Colonies appearing on these plates represent the spontaneous histidine revertants, whose number is characteristic for each strain. The number of spontaneous histidine revertants was subtracted from the total number of colonies on each plate to yield the net number of revertants per dose of sample. Unless otherwise specified, values presented represent the average of at least three experiments incorporating several different doses of test sample tested in triplicate. In accordance with recommendations for Ames testing without microsomal activation (64,65), the

following chemicals were used as positive control agents: 2-nitrofluorene for strain TA98, methyl methane sulfonate for strains TA100 and TA1535, 9-aminoacridine for strain TA1537, 4-nitro-o-phenylenediamine for TA1538. For testing with S-9 microsomal activation, 2-aminoanthracene served as a positive control agent for all strains (63-65). Routine transfer of histidine prototrophs to minimal glucose agar plates was performed in order to confirm that they were actual revertants (64,65). All tests were performed under yellow safe lights to minimize the formation of photoproducts within the samples of soluble organic extract.

Preparation of S-9 Microsomal Fraction

The S-9 microsomal fraction was obtained from the livers of male rats (Sprague-Dawley) which had received a single intraperitoneal injection of Araclor 1245 (Polychlorinated biphenyl) (63,68). All steps were carried out at 0-4°C using sterile solutions, surgical instruments and glassware. Arocolor 1254 at a dosage of 500 mg/kg rat weight was given intraperitoneally; on the fifth day, the rats were sacrificed, their livers removed and weighed, and transferred to a beaker containing 0.15 M KCl (3 mL/g wet liver). The livers were minced with sterile scissors and homogenized in a Waring blender. The homogenate was centrifuged for 10 minutes at 9000 X g and the supernatant (S-9 fraction) decanted, and distributed into 3 dram vials. The vials were quick-frozen in a dry ice-ethanol bath and stored at -70°C until use.

To test the requirement of the sample for metabolic activation, a new vial of S-9 mix was prepared each day, and kept on ice until use. The S-9 mix contains per mL: S-9 (0.1 mL), $MgCl_2$ (8 µM), KCl (33 µM), glucose-6-phosphate (5 µM), NADP (4 µM), and sodium phosphate, pH 7.4 (100 µM) (3). The stock salt solution (0.4 M $MgCl_2$, 1.65 M KCl) and phosphate buffer (0.2 M, pH 7.4) were stored at 4°C. The S-9 mix was filter sterilized through a 0.45 µm Millex filter.

Toxicity Testing

Two different tests were performed to determine the toxicity of the soluble organic extract in the Salmonella tester strains. In the initial test (Toxicity Assay I), nutrient broth was inoculated with either Salmonella strain TA98 or TA100 and incubated with aeration at 37°C for a period of 6 hours. At this time, the extract was added to yield a final concentration of 500 µg/mL. The culture was further incubated at 37°C and at specific time intervals removed, serially diluted in 1 X Spizizen salts and kept at 4°C until 0.1 mL aliquots were plated onto nutrient agar. After a period of incubation (24 hours at 37°C), the number of colonies appearing on the nutrient agar were counted and compared to control cultures which were not exposed to any extract sample. All counts were made on plates having between 30 and 300 colonies. A second toxicity test (Toxicity Assay II) was performed in conjunction with the Quantitative Ames Mutagenicity Test. Overnight cultures (12-16 hrs) of the tester strains used in routine Ames tests were serially diluted in 1 X Spizizen salts and 0.1 mL aliquots of the cells were added to 2.0 mL of top agar, with and without the addition of varying concentrations of the extract sample. The overlays were poured onto minimal glucose agar and incubated for 48 hours at 37°C. After this period of incubation, the ratio of the number of colonies appearing on control and test plates was used to calculate the percentage survival for each of the doses tested. All counts were made with plates having between 30 and 300 colonies.

Bacillus subtilis Comptest

Bacterial Strains and Media

The Comptest system requires the use of B. subtilis strains RUB827 (trpC$_2$, metB10, and polA5) and RUB818 (wild type) (69). RUB827, in addition to being auxotrophic for both tryptophan and methionine, carries two prophages PBSX and Sp . Both of these prophages are inducible following UV-irradiation of RUB827, a process found to be one of the "SOS" phenomena of B. subtilis (70). Competent cells of RUB827 were prepared during successive incubation

periods in growth medium I and growth medium II (71). The Comptest assay was performed on Spizizen minimal medium supplemented with 0.5% glucose and one or both of the amino acids for which RUB827 is auxotrophic. All dilutions of cells were carried out in 1 X Spizizen salts. The genotype of RUB827 was routinely confirmed by demonstrating tryptophan or methionine auxotrophy, and inhibition of growth on 0.05% MMS (polA5 mutation) (70).

Procedures for Genetic Exchange

DNA was isolated from wild type RUB818 and used to transform RUB827 (69,71-73).

Bacillus subtilis Comptest Assay

Cells were grown in GMI for 90 min after the cessation of logarithmic growth, then diluted 10 fold into GMII and incubated for one hour at 37°C on a New Brunswick gyratory shaker at 250 rpm. Following this incubation period, DNA from RUB818 was added to RUB827 (at a final concentration of 1-5 µg/mL and incubation was continued for 25 min. The transformation reaction was terminated with the addition of DNase (100 µg/mL) or by rapid vortexing. The transformed cells were divided into 0.9 mL aliquots and 0.1 mL of the test sample at various concentrations was added. The cells were incubated in the dark with aeration for 30 min. Following this exposure, the cells were centrifuged (800 X g for 2 min), the supernatant discarded, and the pellet resuspended in 1 mL 1 X Spizizen minimal salts. The cells were then plated onto minimal medium supplemented with both or only one of the amino acids for which RUB827 is auxotrophic (tryptophan, methionine). The plates were inverted and incubated at 37°C for 48 hrs. The colonies were scored on the ARTEK counter after 48 hrs of growth at 37°C and duplicate determinations were used for each dose of soluble organic extract in three experiments. The number of transformants was determined from growth in the absence of one of the required amino acids. The total number of viable cells was determined from growth on minimal medium supplemented with both tryptophan and methionine. The relative transformation efficiency (RT) was calculated by

dividing the percentage transformation at a particular dose of the extract by the percentage transformation for cells not exposed to any sample. The reference point of 0.05 RT was used to compare the potency of different samples. Positive control agents MMS and UV-irradiation were routinely tested to demonstrate the presence of inducible prophages.

Toxicity Testing of B. subtilis

The toxicity of the extracts towards B. subtilis strain RUB827 was determined from the Comptest. The colonies appearing on minimal glucose agar supplemented with both tryptophan and methionine are termed "viables." Any decrease in the number of "viables" for cultures receiving doses of the sample is an expression of the toxicity of the samples (69).

RESULTS

Determination of the Mutagenic and "SOS" Inducing Potential of Unextracted Diesel Particulate and the extract.

Ames Mutagenicity Test

The results of the Quantitative Ames mutagenicity test for the extracts and unextracted particle are presented in Table 19. Each sample was tested over a wide dose range. The number of revertants per dose was determined by subtracting the average number of spontaneous revertant colonies appearing on negative control plates from the average number of revertants per plate for each dose tested. The number of revertants per quantity of sample was determined from the slope of the best-fit line through the linear portion of the dose response curve, as calculated by regression analysis. The extract had significant mutagenic activity for strains TA98 and TA100. Microsomal S-9 activation of the extract did not significantly enhance the mutagenic activity of the extract. In fact, in most experiments, the number of revertants per ug of extract actually decreased slightly with the addition of the S-9 fraction. Also the results clearly illustrate the reduced mutagenic activity of

unextracted Diesel particles in comparison to the extract (less than 0.1 revertants per 1.0 mg of particulate matter). Microsomal S-9 activation again did not significantly enhance the mutagenic activity of the sample.

Table 19. Quantitative Ames Mutagenesis Results.

D.P.M from Model Fuel/Air Oxidant	Activity	Revertants/µg TA 98	Activity	TA 100
Unextracted Particles	NAD		NAD	
	NAD	(S-9)	NAD	S-9)
Extract	4.3 ± 0.5		3.2 ± 1.1	
	3.7 ± 0.6	(S-9)	3.3 ± 0.8	(S-9)
Unextracted Particles*	0.11 ± 0.02		0.30 ± 0.12	
	NAD	S-9)	0.14 ± 0.05	(S-9)
Extract*	5.5 ± 1.0		14.9 ± 2.7	

*For comparison purposes the data obtained for an identical engine operating on regular Diesel fuel and lubricant and air oxidant are included.

NAD No Mutagenic Activity Detected.

Bacillus subtilis Comptest

The results of the B. subtilis Comptest for the extracts and unextracted particles are presented in Table 20 (69,73). The competent cultures of strain RUB827 were transformed and exposed to selected doses of either unextracted particles or their extracts. The percentage transformation and the percentage survival of the total population of cells were determined at each dose. The relative transformation efficiency (RT, the percentage transformation of the cells treated with a specific concentration of agent/the percentage transformation of cells not treated) of 0.05 is considered the reference point for the comparison of various samples. A dose response curve for each sample was obtained and from these data, the dose required to reduce the RT to 0.05 was determined. The data clearly demonstrate the reduced DNA damaging activity of unextracted Diesel particles in comparison to the extract. The unextracted particles did not reduce the RT to 0.05 even at doses of 1500 µg/ml.

Table 20. Relative Transformation of Strain RUB827 to Diesel Particulate Matter

DPM from Model Fuel/air oxidant	Average Concentration at which RT = 0.05 (µg/mL)	Percentage Survival at RT = 0.05
Unextracted Particles	NR	97 ± 2
Extract	170 ± 70	68 ± 10
Unextracted Particles*	NR	87 ± 5
Extract*	110 ± 22	55 ± 9

* For comparison purposes the data obtained for an identical engine operating on regular Diesel fuel and lubricant and air oxidant are included.

NR No reduction of RT to 0.05

Toxicity Testing

Salmonella Toxicity Assay II

The results of Toxicity Assay II are presented in Table 21. The number of colonies appearing on the minimal medium receiving selected doses of sample were compared to the number of colonies appearing on minimal medium which did not receive any sample. The extract samples had insignificant toxic effects on strains TA98 and TA100, even at the highest concentrations tested (500 µg per plate). It should be noted that for all of the samples tested in the Ames assay, the mutagenic activity (revertants per µg) was determined at doses not showing significant toxicity. The unextracted particles did not demonstrate significant toxic effects even at a concentration of 1500 µg per plate.

Bacillus subtilis Toxicity Assay

The toxicity of the extracts and unextracted particles to RUB827 were directly determined from the results of the Comptest (Table 20). The colonies appearing on glucose minimal agar supplemented with both tryptophan and methionine are termed "viables." Any decrease in the number of viables for a given dose is an expression of the toxicity of the sample. The percentage toxicity of the extract sample at the concentration which reduces the RT

Table 21. Percentage Survival of TA98, TA100 at Various Doses

DPM from Model Fuel/Air Oxidant	Doses (μg/Plate) 1500 Uneextracted DPM	1000 Unextracted DPM	500 Extract	250 Extract	100 Extract
TA98	79	NT	83	94	NT
TA100	NT	NT	81	91	100
TA98	86*	98*	75*	88*	95*
TA100	NT*	NT*	NT*	NT*	NT*

NT Not tested

* For comparison purposes the data obtained for an identical engine operating on regular Diesel fuel and lubricant and air oxidant are included.

to 0.05 is presented in Table 20. For concentrations reducing the RT to 0.05 but which are not actual test doses, the percentage toxicity was determined at the next highest tested dose. For samples not reducing the RT to 0.05, the percentage toxicity was determined from the results obtained at the highest tested dose. For any of the samples tested, no more than sixty percent of the total cell population was killed by the extract at concentrations which are equal to or greater than required to yield an RT of 0.05.

Biological Activities of Used, Unused Lubricant and Model Fuel

The model fuel and the synthetic lubricant (used and unused) had neither detectable mutagenic activity nor DNA damaging activity, as illustrated by the data in Table 22. Therefore, these compounds have a limited capacity to induce the bacterial "SOS" system. The prototype fuel was tested in increasing volume to volume concentrations up to only 5% because of its greater than ninety-five percent toxicity for the RUB827 at a concentration of 10%. The UCON 525

lubricant was tested in increasing concentrations up to 20% which displayed optimal solubility characteristics.

Table 22. Biological Activity of Used and Unused Lubricant and Model Fuel.

Sample	Revertant per µg of sample TA98	TA100	Conc at which RT equals 0.05 (µg/mL)
Lubricant			
Used	NAD	NAD	NR
Unused	NAD	NAD	NR
Model Fuel	NAD	NAD	NR

NAD No Mutagenic Activity Detected
NR No reduction of RT to 0.05

The Effect of the use of a Nitrogen-free oxidant on the Mutagenic and "SOS" Inducing Activity of Unextracted Diesel Particles and their Extracts

In order to determine the contribution of nitrogen containing compounds to the mutagenic and DNA damaging activities of the compounds present in Diesel exhaust, the particulate matter from the nitrogen-free oxidant was examined. A summary of the biological activity of the unextracted particles and extracts collected without the presence of nitrogen is presented in Table 23.

The results clearly demonstrate the reduced mutagenic activity and DNA damaging activity of extract from particulate generated by a nitrogen-free oxidant. These data illustrate an eight-fold reduction in mutagenic activity following the removal of nitrogen from the engine system. Similarly, there is

a twelve-fold reduction of the mutagenic activity of the extract for TA100 in the absence of nitrogen during the operation of the engine. The mutagenic activity of the extract toward TA98 or TA100 was not enhanced by S-9 microsomal activation. The results of the Comptest clearly demonstrate the reduced DNA damaging activity of the extract generated from the engine operated in the absence of nitrogen. The raw particulate demonstrated neither mutagenic nor DNA damaging activity. The overall toxicity of the extract from the nitrogen-free conditions was less than the toxicity of the extract generated from the engine operated at normal atmospheric conditions. It should be noted, however, that the extract from either system is not sufficiently toxic to interfere with the evaluation of the biological assays.

Table 23. Biological Activity of Particulate Matter Collected from Engine operated with Nitrogen-free oxidant.

Sample	Activity TA98	Revertants/µg TA100	Conc. at which RT equals 0.05 (µg/mL)
Unextracted Particles	NAD(NAD*)	NAD(NAD*)	NR(NR*)
(+S-9)	NAD(NAD*)	NAD(NAD*)	
Extract	0.59±0.5(4.3±0.5*)	0.26±0.2(3.2±1.1*)	NR(170±20*)
(+S-9)	0.32±0.3(3.7±0.6*)	0.16±0.15(3.3±0.8*)	
Percentage Survival	100(83*)	100(81*)	95(68*)

(*) Data obtained with air oxidant
NAD No Mutagenic Activity Detected
NR No reduction of RT to 0.05

Mutagenic Activity of the Diesel Particulate Matter Collected with Different Oxidants.

The biological activities of the extracts of the particulate samples which were collected from the engine operated with different oxidants are shown in Table 24.

Table 24. Biological Activity of Particulate Matter Collected From Engine Operated with Different Oxidants.

Oxidant %	Nitrogen Dioxide (g/IkW-hr)	Particulate Matter (g/IkW-hr)	1-nitropyrene (µg/IkW-hr)	Direct Microbial Mutagenic Activity (Mega Rev/IkW-hr) TA98	TA100
19.1, O_2; 80.9, N_2	0.31	1.69	42.3	1.62	1.36
20.0, O_2; 80.0, N_2	0.45	1.49	23.3	0.73	0.89
21.0, O_2; 79.0, N_2	0.60	1.31	4.5	0.23	0.15
24.8, O_2; 75.2, N_2	1.10	0.61	32.7	1.39	1.23
28.6, O_2; 71.4, N_2	1.01	0.30	20.2	0.74	0.64

These results clearly demonstrate that the observed microbial activity correlates with the 1-nitropyrene concentration. However, other compounds must be contributing to the measured activity since 1-nitropyrene cannot account for all the observed activity. The concentration of 1-nitropyrene can be correlated with the emission rates of particulate matter and of nitrogen dioxide, which are the reactants for the production of 1-nitropyrene.

Mutagenic Activity of the Nitrogen-free Diesel Particulate Matter after Reactions with Nitrogen Dioxide

The biological activities of the extracts of the particulate matter samples which have been reacted with nitrogen dioxide are shown in Table 25.

Table 25. Biological Activity of Particulate Matter After Reaction with Nitrogen Dioxide

Nitrogen Dioxide g/g particles	1-Nitropyrene * µg/g particles	Revertants/µg	
		TA98	TA100
0	0.7	0.12	0.08
0.2	15.4	1.80	NT
1.7	26.6	2.10	1.94
3.5	76.6	2.48	2.08
5.2	86.0	2.60	2.20

NT Not Tested
* These particles contained approximately 400 µg of pyrene/g of particles.

The results clearly demonstrate that the biological activities correlate well with the 1-nitropyrene concentration. However, they also demonstrate that other nitroaromatics must also be contributing to the observed biological activity since the observed activities can not be explained solely on the basis of 1-nitropyrene which has an activity of 400 to 700 revertants/µg (TA98).

CONCLUSIONS

This research project has clearly generated as many questions as it has solved . It has demonstrated that the microbial activity which has been observed for the extract from Diesel particulate matter may be produced by a sampling artifact. Also, since mammalian systems only have nitroreductase in the liver or intestinal tract, the presence of 1-nitropyrene may not represent a real problem. The use of microbial testing systems which do not have the enzyme nitroreductase should be investigated. Also some studies to measure the bioavailability of organic absorbates on the surface of Diesel particulate matter should be made since these studies will define the potential risk of these particles.

References

1. Karim, G. and G. Ward, "The Examination of the Combustion Processes in a Compression-Ignition Engine by Changing the Partial Pressure of Oxygen in the Intake Charge." SAE Paper 680767, 1968.

2. Andon, J., A. Siegel, J. Johnson, D. Leddy, S. Smaby, J. Pitts, A. Winner and K. VanCauwenberghe, "An Initial Assessment of the Literature on the Measurement, Control, Transport, Transformation, and Health Effects of Unregulated Diesel Engine Emissions." National Highway Traffic Safety Administration, January 1979.

3. Ullman, T., K. Springer and T. Baines, "Effects of Six Variables on Diesel Exhaust Particulate." ASME Paper 80-DGP-42, 1980.

4. Tsunemoto, H. and H. Ishitani, "The Role of Oxygen in Intake and Exhaust on NO Emission, Smoke, and BMEP of a Diesel Engine with EGR System." SAE Paper 800030, 1980.

5. Vostal, J., "Health Aspects of Diesel Exhaust Particulate Emissions." Symposium on Health Aspects of Automotive Emissions, May 1980.

6. Lipkea, W., J. Johnson and C. Vuk, "The Physical and Chemical Character of Diesel Particulate Emissions - Measurement Techniques and Fundamental Considerations." SAE Paper SP-430, February 1978.

7. Proceedings of the Scientific Review Meeting on the USEPA Diesel Emission Health Effects Research Program. Arlington, VA, December 1978.

8. Waters, M., S. Nesnow, J. Huisingh, S. Sandhu and L. Claxton, Environ Sci Res, 15, 1978.

9. MacDonald, J., S. Plee, J. O'Arey and R. Schrenk, "Experimental Measurements of the Independent Effects of Dilution Ratio and Filter Temperature on Diesel Exhaust Particulate Samples." SAE Paper 800185, 1980.

10. Bradow, R., "Diesel Particule Emissions." Symposium on Health Aspects of Automotive Emissions, Vol. 56, No. 9, November 1980.

11. Heisey, J. and S. Lestz, "Aqueous Alcohol Fumigation of a Single-Cylinder DI Diesel Engine." SAE Paper 811208, 1981.

12. Campana, J.E., T.H. Risby and P.C. Jurs, Anal Chim Acta, 112:321, 1979.

13. Hansen, G. and B. Munson, Anal Chem, 50:1130, 1978.

14. Baldwin, M.A. and F.W. McLafferty, Organic Mass Spectrom, 7:1353, 1973.

15. Ohasi, M., S. Yamada, H. Kudo and N. Nakayama, Biomed Mass Spectrom 5:578, 1978.

16. Carter F.E., "The Platinum Metals and Their Alloys." Proceedings of the Institute of Metals Division of the American Institute and Mining and Metallurgical Engineers, 1928, pp. 759-85.

17. Tejada S.B., "Analytical Methods for Nitro Aromatic Compounds." In EPA 1981 Diesel Emissions Symposium, U.S. Environmental Protection Agency, Research Triangle Park, North Carolina, 1981.

18. Lee, M.L., D.L. Vassilaros, C.M. White, and M. Novotny, Anal Chem, 51:768, 1979.

19. Funkenbusch, E.F, D.G. Leddy and J.H. Johnson, "The Characterization of the Soluble Organic Fraction of Diesel Particulate Matter." SAE Paper 79418, 1977.

20. Schuetzle, D., F.S. Lee, T.J. Prater, and S.B. Tejeda, Int J Environ Anal Chem, 9:93, 1981.

21. Schuetzle, D., T. Riley, T.J. Prater, T.M. Harvey and D.F. Hunt, Anal Chem, 54:265-272, 1982.

22. Frey J.W. and M. Corn, Nature, 216:615, 1967.

23. Frey J.W. and M. Corn, Am Ind Hyg Assoc J, 28:468, 1967.

24. Lipkea W.H., J.H. Johnson and C.T. Vuk, "The Physical and Chemical Characterization of Diesel Particulate Emissions, Measurement Techniques and Fundamental Considerations." SAE Paper 780108, February 1978.

25. Avgul N.N. and A.V. Kiselev, Chemistry and Physics of Carbon, P.L. Walker, Jr., ed., Vol. 6, No. 1, 1970.

26. Voet A., T.G. Lamond and D. Sweigart, Carbon, 6:707, 1968.

27. Lyon, L.L., G.R. Crocker and J.S. Dahler, Proceedings of the Fourth Carbon Conference, 71, 1960.

28. Nelson, J.R. "Sorption of Organic Molecules into Carbons, Crosslinked Polymers, and Coals of Varying Rank." Ph.D. Thesis, The Pennsylvania State University, 1979.

29. Anderson R.B. and P.H. Emmett, J Appl Phys, 19:367, 1941.

30. Brunauer, S., P.H. Emmett and E. Teller, J Am Chem Soc, 60:309, 1938.

31. Brunauer, S., L.E. Copeland and D.L. Kantro, The Solid-Gas Interface, E.A. Flood, ed., New York: Dekker, 1967.

32. Isirikyan A.A. and A.V. Kiselev, J Phys Chem, 65:601, 1961.

33. Corn, M., T.L. Montgomery and R.J. Reitz, Science, 159:1350, 1968.

34. Ross, M.M., M. R. Chedekel, T.H. Risby, S.S. Lestz and R.E. Yasbin, Environ Int, in press.

35. Brunauer, S., L.S. Deming, W.E. Deming and E. Teller, J Am Chem Soc, 62: 1723, 1940.

36. Zweidinger, R., private communication, U.S. Environmental Protection Agency, Research Triangle Park, North Carolina, 1981.

37. Lowell, S., Introduction to Powder Surface Area: New York, Wiley-Interscience, 1979.

38. Gregg S.J. and K.S.W. Sing, Adsorption, Surface Area, and Porosity, New York: Academic Press, 1967.

39. Pierotti R.A. and R.E. Smallwood, J Coll Interf Sci, 22:469, 1966.

40. Isirikyan A.A. and A.V. Kiselev, J Phys Chem, 66:205, 1962.

41. Babkin, I. Yu. and A.V. Kiselev, Russ J Phys Chem, 36:1326, 1962.

42. Ross, S., J.K. Saelens and J.P. Olivier, J Phys Chem, 66:696, 1962.

43. Elkinton, P.A. and G. Curthoys, J Phys Chem, 73:2321, 1969.

44. Kiselev, A.V., L.A. Migunova and Y.I. Yashin, Russ J Phys Chem, 42:644, 1968.

45. Risby, T.H., R.E. Yasbin and S.S. Lestz, Proceedings of the International Symposium on the Health Effects of Diesel Engine Emission, Vol. 1, 1980, p. 359.

46. Sigsby, J.E., personal communication, U.S. Environmental Protection Agency, Research Triangle Park, North Carolina, 1978.

47. Brunauer, S., L.S. Deming, W.E. Deming and E. Teller, J Am Chem Soc, 62:1723, 1940.

48. Gale, R.L., R.A. Beebe, Russ J Phys Chem, 68:555, 1964.

49. Bradow, R., personal communication, U.S. Environmental Protection Agency, Research Triangle Park, North Carolina, 1978.

50. Kiselev, A.V. and Y.I. Yashin, Gas-Adsorption Chromatography, New York: Plenum Press, 1969.

51. Ingram, D.J.E., Proceedings of the Third Carbon Conference, 93, 1959.

52. Pastor, R.C., J.A. Weil, T.H. Brown and J. Turkevich, Phys Rev, 102:918, 1959.

53. Collins, R.L., M.D. Bell and G. Kraus, J of Appl Phys, 30:56, 1959.

54. Uebersfeld J. and E. Erb, Proceedings of the Third Carbon Conference, 103, 1959.

55. Singer, L.S., Proceedings of the Fifth Carbon Conference, 37, 1963.

56. Petrakis L. and D.W. Grandy, Anal Chem, 50:303, 1978.

57. Singer, H.L., Proceedings of the Fifth Carbon Conference, 37, 1963.

58. Environmental Protection Agency, "Health Effects Associated with Diesel Exhaust Emissions, Literature Review and Evaluation." Springfield VA: National Technical Information Services, November 1978.

59. Lipkea, W.H., J.H. Johnson and C.T. Vuk, "The Physical and Chemical Characterization of Diesel Particulate Emissions, Measurement Techniques and Fundamental Considerations", SAE Paper 780108, February 1978.

60. Pitts Jr., J.N., K.A.V. Cauwenberghe, D. Grosjean, J.P. Schmid, D.R. Fitz, W.L. Belser, Jr., G.B. Knudson and P.M. Knudson, Science 202:515, 1978.

61. Cotton F.A. and G. Wilkinson, Advanced Inorganic Chemistry, 3rd Edition, New York: Wiley-Interscience, 1972, p. 344.

62. Bradow, R.L., Physical and Chemical Characteristics of Diesel Emissions, personal communication. Mobil Source Emissions Resources Branch, Research Triangle Park, North Carolina, 1979.

63. Ames, B.N., J. McCann and E. Yamasaki, Mutat Res, 31:347, 1975.

64. DeSerres, F.J. and M.D. Shelby, Environ Mutagen, 1:87, 1979.

65. DeSerres, F.J. and M.D. Shelby, Science, 203:563, 1979.

66. McCann, J., N.E. Spengarn, J. Kobari and B.N. Ames, Proc Natl Acad Sci, 72:979, 1975.

67. Spizizen, J., Proc Natl Acad Sci, 44:1072, 1958.

68. Czygan, P., H. Green, A.J. Garro, F. Hutterer, F. Schaffner, H. Popper, P. Rosenthal and D.Y. Cooper, Cancer Res, 33:2983, 1973.

69. Yasbin, R.E. and R. Miehl, Appl Environ Microbiol, 39:854, 1980.

70. Yasbin, R.E., Mol Gen Genet, 153:211, 1977.

71. Yasbin, R.E., G.A. Wilson and F.E. Young, J Bacteriol, 121:296, 1975.

72. Dykovich, M., R.E. Yasbin, S.S. Lestz, T.H. Risby and R.B. Zweidinger, Environ Mutagenesis, 3:253, 1981.

List of Publications which have resulted from this research

1. Dukovich, M., "The Mutagenic and "SOS" - Inducing Activity of Diesel Particulate." M.S. Thesis, The Pennsylvania State University, November 1981.

2. Herr, J.D., "Diesel Particulate Emissions from Synthetic Inlet Atmosphere." M.S. Thesis, The Pennsylvania State University, March 1982.

3. Ross, M.M., "Physicochemical Properties of Diesel Particulate Matter." Ph.D. Thesis, The Pennsylvania State Univeristy, August 1981.

4. Yergey, J.A., "Chemical Characterization of Organic Adsorbates on Diesel Particulate Matter." Ph.D. Thesis, The Pennsylvania State University, November 1981.

5. Risby, T.H., R.E. Yasbin and S.S. Lestz, "Diesel Particulate Matter Chemical and Biological Assays." International Symposium on Health Effects of Diesel Engine Emissions, Vol. 1, No. 359, 1980.

6. Dukovich, M., R.E. Yasbin, S.S. Lestz, T.H. Risby and R.B. Zweidinger, "The Mutagenic and Carcinogenic Potential of the Soluble Organic Fraction Collected from Diesel Particulate Emissions." Environ Mutagenesis, 3:253, 1981.

7. Ross, M.M., T.H. Risby, S.S. Lestz and R.E. Yasbin, "Isosteric Heats of Selected Compounds on Diesel Particulate Matter." Environ Sci Technol, 16; 75, 1982.

8. Dukovich, M., R.E. Yasbin, S.S. Lestz, T.H. Risby and J.A. Yergey, "Role of Diesel Fuel Additives in the Mutagenic and Carcinogenic Potential of the Soluble Organic Fraction Extracted from Diesel Particulate Emissions." submitted to Environ Mutagenesis.

9. Ross, M.M., M.R. Chedekel, T.H. Risby, S.S. Lestz and R.E. Yasbin, "Electron Paramagnetic Resonance Spectrometry of Diesel Particulate Matter." Environ Int. in press.

10. Ross, M.M., T.H. Risby, W.A. Steele, S.S. Lestz and R.E. Yasbin, "Physicochemical Properties of Diesel Particulate Matter." Colloids Surfaces, in press.

11. Yergey, J.A., T.H. Risby and S.S. Lestz, "Chemical Characterization of Organic Adsorbates on Diesel Particulate Matter." Anal Chem, 54; 354, 1982.

12. Herr, J.D., M. Dukovich, J.A. Yergey, S.B. Tejada, S.S. Lestz and T.H. Risby, "The Role of Nitrogen in the Observed Direct Microbial Mutagenic Activity for Diesel Engine Combustion in a Single Cylinder DI Engine." SAE, No. 820467, Detroit MI, February 26, 1982.

13. Risby, T.H., R.E. Yasbin and S.S. Lestz, "Diesel Particulate Matter Chemical and Biological Assays." Environ Int, 5:269-279, 1981.